Targeted radionuclide therapy for patients with neuroendocrine tumours

with focus on normal tissue response in ^{177}Lu-DOTATATE treatment

Johanna Svensson

Department of Oncology
Institute of Clinical Sciences
Sahlgrenska Academy at University of Gothenburg

UNIVERSITY OF GOTHENBURG

Gothenburg 2016

Cover illustration: SPECT image of a patient (left), acquired 24 hours after ^{177}Lu-DOTATATE infusion, and tissue sections of kidneys from nude mice; a healthy control (middle) and a damaged kidney (right) after administration of ^{177}Lu-DOTATATE. ©Jens Hemmingsson and Johan Mölne

Targeted radionuclide therapy for patients with neuroendocrine tumours

johanna.svensson@oncology.gu.se

ISBN 978-91-628-9714-7
http://hdl.handle.net/2077/41550

Printed in Gothenburg, Sweden 2016
Ineko

“Whatever turns you on”

-Daniel Norgren

Targeted radionuclide therapy for patients with neuroendocrine tumours

with focus on normal tissue response in ^{177}Lu-DOTATATE treatment

Johanna Svensson

Department of Oncology, Institute of Clinical Sciences
Sahlgrenska Academy at University of Gothenburg
Göteborg, Sweden

ABSTRACT

Targeted radionuclide therapy with ^{177}Lu-DOTATATE for patients with neuroendocrine tumours utilises the frequent overexpressing of somatostatin receptors on the tumour cells. This treatment modality has demonstrated valuable patient benefits and is well tolerated. However, renal and bone marrow toxicity can become dose limiting and persisting. The aim of this thesis was to investigate normal tissue response during ^{177}Lu-DOTATATE treatment, with focus on kidneys, bone marrow and also the spleen, the organ that receives the highest absorbed dose. To enable analysis of bone marrow response to absorbed dose, a novel image-based method for bone marrow dosimetry was developed.

The first paper included, was a pre-clinical study of morphological and biochemical renal changes in nude mice injected with ^{177}Lu-, or ^{90}Y-DOTATATE. The remaining three studies evaluated 51 patients with neuroendocrine tumours, treated with ^{177}Lu-DOTATATE at Sahlgrenska University Hospital. Patient renal and bone marrow function was evaluated and dosimetry was performed for kidneys, bone marrow and spleen utilising planar and SPECT images acquired after infusion, and the developed automated segmentation method for bone marrow dosimetry.

Selective morphological changes were quantified in renal cortex of nude mice, and corresponding biochemical changes observed, after ^{177}Lu-DOTATATE injection. These appeared in a dose-dependent manner. No morphological changes were observed for the animals receiving ^{90}Y-DOTATATE. In the clinical studies, it was found that patients with inferior renal function were exposed to higher mean absorbed renal doses, and experienced enhanced haematological toxicity. It was also shown that a longer residence time for ^{177}Lu and a higher tumour burden increased the haematological toxicity. A novel image-based method for bone marrow

dosimetry was developed, and correlations were found between mean and total absorbed bone marrow doses, and haematological toxicity. The role of the spleen for haematological toxicity was also analysed, and it was observed that radiation exposure of the spleen had an impact on the haematological response. The results in this thesis emphasise that several parameters affects normal tissue response in ^{177}Lu-DOTATATE treatment. Hopefully, a better understanding of what decides the individual response, may contribute to individualised treatment decisions in the future.

Keywords: radionuclide therapy, ^{177}Lu-DOTATATE, neuroendocrine tumours, normal tissue response, dosimetry

ISBN: 978-91-628-9714-7

SAMMANFATTNING PÅ SVENSKA

Radionuklidterapi med ^{177}Lu-DOTATATE är ett viktigt behandlingsalternativ för patienter med neuroendokrina tumörer som överuttrycker somatostatinreceptorer. En majoritet av patienterna har nytta av behandlingen och effekten är ofta långvarig. Toleransen är generellt god men även normalvävnaden bestrålas, och dosen till framför allt njurarna och benmärgen kan ge allvarliga biverkningar på kort och lång sikt. Syftet med denna avhandling var att studera normalvävnadens reaktion på bestrålningen vid ^{177}Lu-DOTATATE behandling, med fokus på njurar, benmärg och även mjälten, som är det organ som erhåller högst stråldos.

Det första arbetet, som var prekliniskt, analyserade njurar samt blodprover från nakna möss efter injektion med ^{177}Lu- eller ^{90}Y-DOTATATE. I de följande arbetena utvärderades 51 patienter behandlade med ^{177}Lu-DOTATATE vid Sahlgrenska Universitetssjukhuset. Njur- och benmärgsfunktion följdes och medelabsorberad dos till njurar, benmärg och mjälte beräknades med information från upprepade bildtagningar efter behandlingen. En ny, bildbaserad metod för beräkning av benmärgsdos utvecklades.

Dosberoende njurpåverkan kunde konstateras såväl morfologiskt som biokemiskt hos mössen som injicerats med ^{177}Lu-DOTATATE, och syntes drabba proximala tubuli i cortex selektivt. Inga tecken på njurpåverkan sågs hos djuren som erhållit ^{90}Y-DOTATATE. I de kliniska arbetena noterades att patienter med sämre njurfunktion exponerades för högre njurdos vid behandling. Dessa patienter drabbades också av allvarligare hematologisk toxicitet. Patienternas tumörbörda och residenstid för ^{177}Lu analyserades, och båda dessa faktorer påverkade den hematologiska toxiciteten. Absorberad dos till benmärg beräknades med den nya metoden, och en korrelation sågs till hematologisk respons. Mjältens exponering undersöktes också, och en viss korrelation sågs mellan mjältdos och hematologisk respons.

Stråldosen till benmärg och mjälte korrelerade således med hematologisk respons. Variationen var emellertid stor, beroende på att flera kliniska faktorer såväl som den individuella strålkänsligheten påverkar respons hos exponerade organ. Kunskapen om vilka faktorer som påverkar normalvävnadsrespons ger förutsättningar att finna metoder för att väga samman dessa, och tidigt förutsäga tolerans och därmed kunna individanpassa behandlingen.

LIST OF PAPERS

This thesis is based on the following studies, referred to in the text by their Roman numerals.

I. Svensson, J, Mölne, J, Forssell-Aronsson, E, Konijnenberg, M, Bernhardt, P. Nephrotoxicity profiles and threshold dose values for ^{177}Lu-DOTATATE in nude mice. Nuclear Medicine and Biology 2012; 59: 756-762.

II. Svensson, J, Berg, G, Wängberg, B, Larsson, M, Forssell-Aronsson, E, Bernhardt, P. Renal function affects absorbed dose to the kidneys and haematological toxicity during ^{177}Lu-DOTATATE treatment. European Journal of Nuclear Medicin and Molecular Imaging 2015; 42: 947-955.

III. Svensson, J, Magnander, T, Hagmarker, L, Hemmingsson, J, Wängberg, B, Bernhardt, P. A novel planar image-based method for bone marrow dosimetry in ^{177}Lu-DOTATATE treatment correlates with haematological toxicity. Submitted 2016-02-28.

IV. Svensson, J, Hagmarker, L, Magnander, T, Wängberg, B, Bernhardt, P. Radiation exposure of the spleen in ^{177}Lu-DOTATATE treatment and its relation to haematological toxicity and volume reduction of the spleen. Submitted 2016-02-28.

RELATED PRESENTATIONS

1. Svensson, J, Schmidt, A, Wikström, A, Forssell-Aronsson, E, Mölne, J, Konijnenberg, M, Bernhardt, P. Equal mean absorbed kidney dose from ^{177}Lu-DOTATATE and ^{90}Y-DOTATATE will generate different kidney toxicity profiles in nude mice. European Association of Nuclear Medicine (EANM), Barcelona; 2009 (oral presentation)
2. Svensson, J, Schmidt, A, Wikström, A, Forsell-Aronsson, E, Mölne, J, Konijnenberg, M, Bernhardt, P. ^{177}Lu-DOTATATE and ^{90}Y-DOTATATE will generate different kidney toxicity profiles in nude mice. Läkarstämman, Stockholm; 2009 (poster)
3. Konijnenberg, M, Melis, M, De Jong, M, Bernhardt, P, Svensson, J. Dose distribution models in mice kidneys for ^{90}Y, ^{111}In or ^{177}Lu; a valuable tool for biological effective dose estimate. EANM, Wien; 2010 (poster)
4. Svensson, J, Hermann, R, Forssell-Aronsson, E, Wängberg, B, Bernhardt, P. Impairment in renal function predicts high kidney uptake of radiolabelled somatostatin analogues in treatment of patients with neuroendocrine tumours. EANM, Milan; 2012 (poster)
5. Svensson, J, Hermann, R, Forssell-Aronsson, E, Wängberg, B, Bernhardt, P. Does impairment in renal function predict higher mean absorbed kidney doses in peptide receptor radionuclide therapy? Cancerfondens planeringsgrupp för radionuklidterapi, Stockholm; 2012 (oral presentation)
6. Sundlöv, A, Svensson, J, Sjögreen Gleisner, K, Ljungberg, M, Bernhardt, P, Hindorf, C, Mortensen, N, Morin, K, Hermann, R, Wängberg, B, Ohlsson, T, Forssell-Aronsson, E, Tennvall, J. A Phase II Trial of Dose Escalation in ^{177}Lu-DOTATATE PRRT - the Need for Dosimetry. EANM, Göteborg; 2014 (oral presentation)
7. Svensson, J, Söderström, J, Magnander, T, Wikberg, E, Wängberg, B, Bernhardt, P. An image based method for bone marrow dosimetry in ^{177}Lu-DOTATATE therapy. EANM, Hamburg; 2015 (oral presentation)

CONTENT

ABBREVIATIONS

α	Alpha particle (Helium nucleus)
Arg	Arginine
β	Beta particle (electron)
BED	Biologically effective dose
CR	Complete remission
Cg A	Chromogranin A
DOTA	Dodecane tetraacetic acid
DOTANOC	DOTA, 1-NaI^{3}-octreotide
DOTATATE	DOTA, Tyr^{3}-octreotate
DOTATOC	DOTA, Phe^{1}-Try^{3}-octreotide
DTPA	Diethylene triamine pentaacetic acid
E_{mean}	Mean energy per decay
γ	Gamma ray (electromagnetic radiation)
LET	Linear energy transfer
LQ	Linear-quadratic model
Lys	Lysine
MIRD	Medical internal radiation dose
NCI CTCAE	The National Cancer Institute Common Toxicity Criteria of Adverse Events
NET	Neuroendocrine tumour

NTCP	Normal tissue complication probability
PET	Positron emission tomography
PhONSAi	The medical Physics, Oncology, and Nuclear medicine research image platform at Sahlgrenska Academy
PR	Partial remission
PRRT	Peptide receptor radionuclide therapy
RFA	Radiofrequency ablation
R_{mean}	Mean range per decay
SD	Stable disease
SI-NET	Small intestinal neuroendocrine tumour
SPECT	Single-photon emission computed tomography
SSTR	Somatostatin receptor
TAE	Transarterial embolisation
TACE	Transarterial chemoembolisation
TARE	Transarterial radioembolisation
$t_{½}$	Physical half-time
V_{mean}	Mean volume

1 INTRODUCTION

This thesis explores important aspects of the normal tissue response to peptide receptor radionuclide therapy (PRRT) with focus on ^{177}Lu-DOTATATE, a therapy that has become an established treatment option for patients with advanced neuroendocrine tumours that overexpress somatostatin receptors.

1.1 Neuroendocrine tumours

Neuroendocrine tumours (NETs) develop from neuroendocrine cells throughout the body [1]. The most common sites of origin are the respiratory tract, the gastrointestinal canal and endocrine pancreas. Neuroendocrine cells regulate respiratory function in the respiratory tract and gastrointestinal motility and secretion in the gastrointestinal canal. In the pancreas they release hormones such as insulin, gastrin and glucagon. Some tumours that originate from neuroendocrine cells overproduce peptides or hormones, giving rise to specific symptoms. Most characteristic is the carcinoid syndrome, in which small intestinal NETs (SI-NETs) overproduce amines and peptides, resulting in diarrhoea, flushing and sometimes tricuspid and pulmonary heart valve disease and bronchoconstriction [2, 3].

Published epidemiologic data show that the incidence of NETs has increased over the past 40 years in most areas, including Western Europe, North America and Japan [4-7]. The largest series of published patients (n=35 825) is from the Surveillance, Epidemiology, and End Results (SEER) Program of the National Cancer Institute in the United States. They reported an increase from 1.09 cases per 100,000 in 1973 to 5.25 cases per 100,000 in 2004 [4]. This increase is thought to be due to more accurate diagnostics and reporting of these relatively rare malignant diseases, but it is possible that there has been a true increase in NET incidence.

The most common primary site of NET varies to some extent with sex and race [4]. Women and men are affected equally, and the prevalence of NETs is reported to be 35 per 100 000. These tumours are classified based on the proportion of proliferating tumour cells in the tumour as determined by the proliferation marker Ki-67 [8]. NETs with a Ki-67-index of 0−2% are classified as Grade 1 (G1), those with 3−20% as Grade 2 (G2), and NETs with >20% as Grade 3 (G3) [9]. The median overall survival time is 75 months, but the prognosis varies according to the origin, stage and grade of

disease. For example, patients diagnosed with G1 NETs have a median overall survival time of over 10 years, while the median overall survival time for patients with G3 NETs is less than one year [4].

1.1.1 Diagnosis of neuroendocrine tumours

NETs are often characterised by an indolent course of disease. Patients may have non-specific gastrointestinal symptoms, resulting in delayed diagnosis. However, those with functional tumours, that overproduce hormones and bioactive peptides, develop symptoms due to the action of the specific hormone or peptide. Examples include hypoglycaemia from insulin overproduction, multiple peptic ulcers from gastrin overproduction and Cushing´s syndrome due to ACTH overproduction from a pancreatic NET. SI-NETs often produce serotonin and peptides that causes the carcinoid syndrome as described above. This hormonal overproduction may also cause fibrosis in the tricuspid and pulmonary heart valves and around mesenteric and retroperitoneal tumours. This occasionally leads to heart insufficiency, impaired bowel circulation and bowel obstruction, respectively. However, many NETs are non-functioning, and are detected as other solid tumours, i.e. when they give rise to local symptoms.

NET diagnosis is based on structural imaging by CT or MRI, which is usually complemented with somatostatin receptor imaging (see Section 1.3). Biochemical screening includes determination of the serum level of the non-specific neuroendocrine tumour marker chromogranin A, which is typically elevated, and urine or serum levels of peptides or amine metabolites, e.g. the serotonin metabolite 5-HIIA in SI-NETs. Sometimes screening includes an analysis of pancreas-specific hormones, such as gastrin, insulin and pancreatic polypeptide. The choice of markers depends on the symptoms and on the location of the primary tumour, if it is known. Histopathologically, well differentiated neuroendocrine tumour cells are relatively uniform and contain neurosecretory granules. The cells are also characterised by positive staining for chromogranin A and synaptophysin [10].

1.1.2 Treatment of neuroendocrine tumours

The primary treatment for NETs is surgery, which may be sufficient to cure patients with localised or loco-regional disease. The SEER database shows that 59% of patients diagnosed with NETs in the United States between 1973 and 2004 were classified into these groups [4]. If the disease has spread, the liver is the most common site of metastases. For liver-dominant disease, regional treatment of liver metastases is well established and includes radiofrequency ablation (RFA), transarterial embolisation (TAE),

transarterial chemoembolisation (TACE) and transarterial radioembolisation (TARE) [11]. Systemic treatment is needed for disseminated disease that includes tumour sites outside the liver. The development of systemic treatment alternatives has been challenging, as the disease often is indolent with only a smaller percentage of tumour cells proliferating. A few subgroups of NETs, such as pancreas-derived NETs, are sensitive to chemotherapy [12] or to targeted therapy such as tyrosine kinase or mTOR inhibitors [13, 14]. It was recently established that targeting of the often overexpressed somatostatin receptors on the tumour cells not only provide symptom relief by reducing amine and peptide secretion [15], but also have antiproliferative effects [16, 17].

1.2 Somatostatin receptors

Somatostatin receptors (SSTRs) are expressed throughout the body. A majority of NETs overexpress SSTRs [18], which comprise a family of G protein-coupled transmembrane receptors. Five subtypes have been identified, termed SSTR1-SSTR5 [19]; and of these, SSTR-2 is the most frequently overexpressed receptor for a majority of NETs [20]. The natural ligands for these receptors are the somatostatin-14 and somatostatin-28 peptides. Somatostatin acts as an inhibitor of motility, exocrine secretion, and peptide and hormone secretion in the gastrointestinal tract. After the discovery that SSTRs are often overexpressed on neuroendocrine tumour cells, patients were treated first with natural somatostatin and later with the more stable somatostatin analogue octreotide; these agents helped mitigate peptide or hormone-related symptoms [21]. Based on these observations, a development of imaging and therapy modalities based on SSTR overexpression started.

1.3 Somatostatin receptor imaging and therapy using radionuclides

The high level of SSTR expression on neuroendocrine tumour cells has allowed the development of SSTR imaging modalities that use radionuclides to visualise the tumours, as well as to SSTR-based radionuclide therapy. Imaging of SSTR-positive tumours was first demonstrated using an ^{123}I-labeled somatostatin analogue [22], but soon ^{111}In-labeled octreotide, stabilised by the chelating agent diethylene triamine pentaacetic acid (DTPA), was established as the diagnostic tool of choice for the diagnosis and staging of NETs [23]. Dodecane tetraacetic acid (DOTA) later replaced DTPA as a chelator after biodistribution studies compared the two

compounds [24]. ^{111}In can be used for imaging because of its γ-component, but it was also investigated as a potential therapeutic agent since it emits high linear energy transfer (LET) Auger electrons. Although this agent provided symptom relief and elicited a biochemical response [25, 26], further study of ^{111}In-based SSTR therapy showed only modest radiological responses. This is probably due to that the radiopharmaceutical did not reach the nucleus of the tumour cell, which is needed for the short-range Auger electrons to have an effect. Instead β-emitting radionuclides, such as ^{90}Y and ^{177}Lu, were found to be more suitable for SSTR-based therapy.

Octreotide was the first somatostatin analogue developed for both diagnostic and therapeutic use. Subsequent pre-clinical and clinical studies demonstrated that after octreotide was modified to octreotate by replacing the C-terminal threoninol with threonine, its binding to SSTR-positive tissues improved because of a higher affinity for SSTR-2 [27-29]. The biodistribution of the radiopharmaceutical has several important aspects, including its tumour-to-blood uptake ratio, normal tissue uptake and whole-body clearance. It is desirable to have a prolonged tumour cell uptake of the radiopharmaceutical for imaging purposes and for the agent to exert its therapeutic effects. This is accomplished with both ^{111}In-DOTA-octreotide (^{111}In-DOTATOC) and ^{177}Lu-DOTA-octreotate (^{177}Lu-DOTATATE), because they are internalised [30-32]. However, this must be balanced by considering tolerable normal tissue uptake and retention.

The β-emitters ^{177}Lu and ^{90}Y dominate SSTR-based therapy, but the first clinical experiences with α-emitters have been reported. Treatment with ^{213}Bi-DOTATOC showed tumour responses in patients who were refractory to ^{177}Lu-/ ^{90}Y-DOTATATE-based therapy [33]. The high-LET α-emission from ^{213}Bi and its short range in tissue is thought to make it suitable mainly for microscopic disease, but the above mentioned study reported tumour response in manifest metastases. The high LET of α-emitters implies a risk of pronounced toxicity in dose-limiting organs, depending on the radiosensitivity of the tissues that accumulate the radiopharmaceutical. Although this was not observed in that study; its safety and efficacy profile needs to be studied further. The short half-life (45.6 min) of ^{213}Bi may prevent a sufficiently high tumour-to-normal tissue activity concentration ratio, a factor showed to affect the efficacy of β-emitters [34].

Positron emission tomography (PET) has been developed for imaging NETs for diagnostic, staging and treatment purposes, using ^{68}Ga coupled to a somatostatin analogue via DOTA. PET-based imaging, which is complemented by CT scanning, has shown greater sensitivity in detecting

NET lesions because of the higher image resolution compared to SPECT [35, 36]. Three different somatostatin analogues are used and coupled to DOTA, namely DOTATOC, DOTATATE and DOTANOC. No clinically relevant differences in sensitivity have been observed between them [37-41]. ^{68}Ga-based PET imaging seems superior to the well established ^{18}F-FDG PET in tumour diagnostics for most lower grade NETs (G1 and G2) [42, 43]. This high-resolution imaging allows detailed mapping of ^{68}Ga-labeled somatostatin analogue uptake, both physiological and pathological; accordingly, there is a need for methods that distinguish benign tissues from tumours with high specificity [44].

1.3.1 Properties of ^{177}Lu and ^{90}Y

The radionuclides that are most often used for somatostatin analogue-based peptide receptor radionuclide therapy (PRRT); β-emitting ^{177}Lu and ^{90}Y, are suitable for systemic radionuclide therapy because of their physical properties. ^{177}Lu is a low-medium energy β-emitting radionuclide (E_{mean}=147 keV) with a physical half-life of 6.7 days. It also emits γ-rays (E=113 keV and 208 keV), so it can be detected and quantified by gamma camera imaging. ^{90}Y is a pure high-energy β-emitter (E_{mean}=934 keV) with a physical half-life of 2.7 days [45, 46]. With a maximum-range for the β-particles of 1.8 mm, ^{177}Lu may be more effective in the treatment of smaller tumours (<1 g) while ^{90}Y, with a maximum-range of 11 mm, is better suited for larger tumours, and might be able to more effectively compensate for heterogeneous activity distribution [34, 47].

1.3.2 Preparation of ^{177}Lu-DOTATATE

The radiolanthanide ^{177}Lu is produced by neutron irradiation of ^{176}Lu or ^{176}Yb in a nuclear reactor [48, 49]. Octreotate is coupled to DOTA upon delivery to the hospital, and then DOTA-octreotate (DOTATATE) is labeled with ^{177}Lu on the day of treatment [29, 50]. The amount of peptide that is added is critical, as this can affect uptake by both the tumour and by normal tissue [48, 51, 52]. Most reports label 200 μg of DOTATATE with 7.4 GBq of ^{177}Lu [51]. The radiochemical yield and purity is determined by instant thin-layer chromatography (ITLC), and the fraction of peptide-bound ^{177}Lu must be high (≥98%) to prevent free ^{177}Lu from circulating and possibly accumulating in the bone marrow and other tissues [53]. In order to reduce the free fraction of ^{177}Lu after the labeling procedure and to ensure quality control, unbound DTPA can be added that will form a complex with ^{177}Lu [53].

1.3.3 ^{177}Lu-DOTATATE treatment

Most clinical protocols use 3.7 or 7.4 GBq of ^{177}Lu-DOTATATE for each treatment fraction [54-58]. The radiopharmaceutical is administered as an intravenous infusion over 30 minutes in 100 ml of 0.9% NaCl. To minimise physiological renal uptake of the radiolabeled peptide, positively-charged amino acids are co-infused to provide competitive inhibition. Most reported protocols use the basic amino acid lysine (2.5%), either alone or in combination with arginine (2.5%), in 1000 ml of 0.9 % NaCl, administered at an infusion rate of 250 ml/h, starting 30 minutes before the infusion of the radiopharmaceutical [59, 60]. Prolonged infusion of amino acids and more intense hydration may improve renal protection [61, 62]. Treatment with long acting somatostatin analogues is interrupted 4−6 weeks before each fraction to avoid saturation of SSTRs.

^{177}Lu-DOTATATE treatment can be performed in an outpatient setting, depending on national radiation protection regulations, but most often the patients stay at the hospital overnight. It is usually given in repeated fractions at intervals of 6 to 10 weeks to allow the bone marrow and other normal tissue to recover. The number of fractions, i.e. the total amount of radiopharmaceutical that is delivered, is most often restricted by a mean absorbed renal dose of 23-28 Gy, or by a mean absorbed bone marrow dose of 2 Gy [57, 60].

1.4 ^{177}Lu-DOTATATE dosimetry

Because ^{177}Lu emits γ-radiation it is possible to locate the radiopharmaceutical and to quantify organ and tumour uptake after its injection using a gamma camera to perform planar and single-photon emission computed tomography (SPECT) imaging. Repeated planar imaging and a SPECT acquired 24 hours post-injection (p.i.) in conjunction with CT, reveals the kinetics of ^{177}Lu biodistribution and the volumes of the tissues that accumulate activity. This makes it possible to estimate the absorbed doses. For accurate absorbed dose-estimates, frequent imaging is needed to capture the dynamics of the uptake and elimination phases [63]. In clinical practise, 3 or 4 time points are usually chosen for imaging, typically 1−2, 24 and 48 hours p.i. plus one later time point, typically 96 to 168 hours p.i. [50, 57]. A late time point is critical to accurately estimate the total exposure; otherwise, there is a risk of overestimating or underestimating the activity [50, 64, 65].

The conjugate-view method is the most commonly used method for quantifying the activity of the administered radiopharmaceutical. A region of interest (ROI) is drawn around the organ or tumour in the planar anterior and posterior gamma camera images, and the background-corrected counts in the ROI are converted to activity using the equation:

$$A = \frac{\sqrt{C_A C_p} \cdot e^{\frac{\mu T}{2}} \cdot \mu t}{k(1-e^{-\mu t}) \cdot e^{\frac{\mu t}{2}}} \qquad \text{(Eq. 1)}$$

Here, T is the thickness of the body over the organ, and t is the thickness of the organ of interest. The effective attenuation coefficient, μ, and the sensitivity factor, k, can be determined by scintigraphy of a planar ^{177}Lu source equal to the cross-sectional area of the organ to be estimated. The source is placed at different depths in a phantom of tissue equivalent material and quantified [57].

When the activity has been quantified at the different time points, a time-activity curve is created, and the accumulated activity can be estimated from the area under the curve. The absorbed dose from the emitted electrons is then calculated using the equation:

$$D = \frac{\tilde{A} \cdot \Delta \cdot \varphi}{M} \qquad \text{(Eq. 2)}$$

In this equation, $\tilde{A}$ is the accumulated activity in the organ, Δ is the total electron energy emitted by the radionuclide per disintegration (147 keV for ^{177}Lu; [45]), φ is the absorbed fraction of energy from the electrons, and M is the mass of the organ. If there is an assumption of local absorption of emitted electrons, the absorbed fraction φ will be 1. The energy deposition from γ-radiation from inside the organ and from source organs outside the target organ can be neglected, assuming only a minor contribution from photons in organs with high uptake of the radiopharmaceutical and low abundance of photon emission ($\leq$2% of the absorbed dose for ^{177}Lu; [50, 66].

SPECT imaging, which is usually performed 24 hours p.i., can be used to complement the activity data acquired from the planar images. The calculated activity in the organ of interest is then used to adjust the time-activity curve acquired from the planar images, as a ”hybrid” method of two-dimensional (2D) and three-dimensional (3D) dosimetry [67]. Pure 3D dosimetry is also utilised with frequent SPECT imaging to quantify radionuclide uptake and follow its kinetics [68].

1.4.1 Bone marrow dosimetry

It is challenging to use image-based activity quantification to estimate the absorbed dose to the bone marrow. This organ is not easily detected or quantified by imaging because of its generally low specific uptake of ^{177}Lu, and its distribution in the bones of the trunk.

It is possible to directly measure the activity concentration using bone marrow aspiration [69], but this does not describe the kinetics or the regional differences in uptake, and frequent sampling is not practicable. Instead, indirect methods are used to estimate the absorbed dose to the bone marrow (Table 1). These methods include frequent blood sampling and estimation of the activity concentration and the kinetics in blood after infusion of the radiopharmaceutical [70]. The relationship between the activity concentration in the bone marrow and in the blood must then be determined. In radionuclide therapy that uses intact antibodies, the ratio between the two compartments is considered to be around 0.3 [71], but the biodistribution of the much smaller peptides used for PRRT (1 kD vs. 150 kD), is different, and the ratio is estimated to be close to 1 [63, 69, 72].

After the activity concentration in the bone marrow has been calculated for the different time points, time-activity curves can be created and the accumulated activity determined. To estimate the absorbed dose from the electrons emitted from the bone marrow (self-dose), the absorbed fraction and the mass needs to be known. As noted earlier, the absorbed fraction may be set to 1, and a mean value for the bone marrow mass can be calculated from a reference male or female and then adjusted by the patient´s weight [73]. To determine the total absorbed dose, the contribution from photons in the remaining parts of the body needs to be added. This is accomplished by quantifying the accumulated activity in the planar images collected p.i.

Jackson et al. described a method for a pure image-based estimation of bone marrow activity that utilises frequent SPECT imaging (Table 1; [74]). A potential association with haematological response was not reported.

Table 1. Studies on blood and image-based bone marrow dosimetry in ^{177}Lu-DOTATATE treatment

Author, year	Patients, n	Method	BM dose (Gy/7.4 GBq)
Wehrmann, 2007	27	Blood, imaging	0.30
Forrer, 2009	13	Blood, urine, imaging	0.25
Bodei, 2011	12	Blood, imaging	0.25
Sandström, 2013	200	Blood, urine, imaging	0.12 median
Jackson, 2013	28	Imaging	0.11−0.26
Bergsma, 2016	23	Blood, urine, imaging	0.50

1.4.2 Accuracy of 2D and 3D dosimetry

Planar (2D) dosimetry was the first established method, and is probably still the most used method, for ^{177}Lu-DOTATATE treatment. This method has several uncertainties, including activity from over- and underlying organs and tumours, and the background correction is critical [75, 76]. The effective attenuation and the sensitivity of the camera can be determined, but these can still add further uncertainty to the absorbed dose estimation. 3D dosimetry using SPECT is superior in terms of activity determination because the uptake in the volume of interest can be quantified separately. However, photon attenuation, as well as the contribution from scattering in the subject, must be taken into consideration in both modalities. Even though 3D imaging can be repeated (just like 2D) to follow the kinetics and to calculate the dose, the information from SPECT imaging is limited by the field of view, the resolution of the camera, and the partial volume effect, especially for smaller objects [77, 78]. Examples of experimentally determined recovery factors were published recently for ^{177}Lu-DOTATATE SPECT imaging in order to correct for the partial volume effect [68, 79].

In current practise, both 2D and 3D dosimetry are usually performed for absorbed dose estimates in ^{177}Lu-DOTATATE treatment, although some centres use only 3D dosimetry. Comparing the two shows that 2D dosimetry has a risk of overestimating the activity [66, 67], while 3D dosimetry is considered more accurate [80, 81].

1.4.3 Dosimetry of ^{90}Y-DOTATOC/TATE

Dosimetry for ^{90}Y-DOTATOC/TATE has other prerequisites, as ^{90}Y is a pure β-emitter. Accordingly, for ^{90}Y pre-therapeutic absorbed dose estimates can

be performed using the positron emitter ^{86}Y or γ-emitting ^{111}In [82-84]. This approach has some uncertainties because the radionuclides have different physical properties, and the biodistribution may vary. The choice of different time points for dosimetry and therapy can also be a source of uncertainty. Nevertheless, a study by Barone et al. showed a clear dose-response relationship between the estimated absorbed renal doses from ^{86}Y-based dosimetry and long-term renal response (yearly loss in creatinine clearance) [85]. The choice of somatostatin analogue is also important for accuracy, as the affinity to the SSTRs varies [86].

1.5 Efficacy of ^{177}Lu-DOTATATE

In the past there were only a few treatment options for most patients with advanced NETs, so somatostatin analogue-based PRRT represents an important advancement in the management of the disease. The first larger study, performed in Rotterdam in 2005, reported that 131 patients treated with ^{177}Lu-DOTATATE showed more favourable response rates than earlier reported from chemotherapy, with a disease control rate (CR+PR+SD) of 82% [60]. Randomised studies are still missing though. The time to disease progression was reported to be more than 36 months for the responding patients in this study. These results were promising, even though all patients were not progressing at time of treatment, and the disease is known to be very slow growing sometimes. Subsequently other centres in Europe and throughout the world reported similar experiences with ^{177}Lu-DOTATATE in terms of response rate and duration of response, also for patients with established disease progression [61, 87]. Another important effect of the treatment is that patients reported symptom relief and improvement in their quality of life [61, 88]. The response rates and the duration of response for ^{90}Y-DOTATOC/TATE are reported to be similar to those for ^{177}Lu-DOTATATE [89, 90].

Few studies have investigated the dose-response relationship between the absorbed tumour dose and tumour shrinkage. This is probably due to the difficulties in estimating the absorbed dose. First, there are only a few data points from post-therapeutic images for the kinetics of the radiopharmaceutical, and second, SPECT images has limited spatial resolution. However, one study of ^{90}Y-DOTATOC showed a dose-response relationship using ^{86}Y-DOTATOC for PET-based dosimetry [84]. And recently, a study of ^{177}Lu-DOTATATE also showed a dose-response relationship [68]. Here, the correlation was stronger for lesions larger than 4

cm in diameter, probably because there was less of a partial volume effect than for the smaller (2.2−4 cm) lesions (R^2 0.91 vs. 0.64).

Progressive disease is reported to have an impact on treatment efficacy [61], while tumour burden, bone metastases, previous chemotherapy, Ki-67 proliferation index and performance status at baseline have all been reported to affect survival [54, 61, 87]. The combination of ^{177}Lu-DOTATATE and ^{90}Y-DOTATOC/TATE is being evaluated to improve treatment efficacy by taking advantage of their different physical properties. One study (n=50) compared ^{90}Y-DOTATATE alone to the combination of ^{90}Y and ^{177}Lu, and the combination arm had superior overall survival [91]. The patients were not randomised, however, and the absorbed tumour doses were not comparable between the groups.

1.6 Side-effects of ^{177}Lu-DOTATATE

Treatment with ^{177}Lu-DOTATATE is generally well tolerated, and it is possible to administer the treatment on an outpatient basis if it is allowed by national radiation protection regulations. The most common acute side effect is nausea, which is reported by about 25% of patients. Vomiting, abdominal discomfort or pain, mild asthenia and temporary hair loss have also been observed [54, 61], as has liver toxicity in a few cases [54].

Efforts to limit the side effects of ^{177}Lu-DOTATATE have focused on the kidneys and the bone marrow, which are the two major dose-limiting organs. Less focus has been on the spleen, the organ that is exposed to the highest mean absorbed doses [61], due the presence of SSTRs [92], and a subsequent relatively high physiological uptake.

1.6.1 Renal uptake and toxicity

The exposure of the kidneys to radiation during ^{177}Lu-DOTATATE treatment is due to active reabsorption and retention of the radiolabeled peptide (octreotate) in the proximal tubules via the endocytic megalin and cubulin receptors. This was confirmed directly in studies on megalin-deficient rats and mice [93, 94] and indirectly in human studies that used renal ex vivo autoradiography [95]. Uptake in the kidneys may also be due to some extent to the presence of SSTRs [96, 97], even though their role in renal exposure during ^{177}Lu-DOTATATE treatment has not been evaluated.

The amount of treatment is usually restricted by a fixed absorbed dose limit to the kidneys, to avoid serious acute or long-term impairment. An absorbed

dose limit of 23 or 28 Gy was originally based on what was known about renal tolerance to external radiotherapy using a normal tissue complication probability (NTCP) of 5% or 50% after 5 years [98]. The linear-quadratic (LQ) model was developed to compare radiotherapy delivered using different fractionations and dose rates and targets (tumours and organs at risk) with different radiosensitivities [99]. The LQ model was later adopted for use with radionuclide therapy [100] and applied to renal tolerance for PRRT. Two studies found biologically effective dose (BED) limits of 28 Gy for patients with risk factors for renal impairment (hypertension, diabetes), and 40 Gy for patients without risk factors [101, 102].

Several methods are used to estimate renal function (creatinine, creatinine clearance, ^{99m}Tc-DTPA), and the methods are difficult to compare; nevertheless the frequency of complications is low. Serious renal toxicity (Grade 3−4 according to NCI CTCAE) is rarely observed during ^{177}Lu-DOTATATE treatment [54, 55], and the prevalence in long-term follow-up is also low. A yearly loss in glomerular filtration rate (GFR) of 2% have been reported in long term follow-up, as has renal toxicity grade 3–4 in 0–3% of patients [54, 55, 103].

The kidneys are affected more often with ^{90}Y-DOTATOC/TATE treatment than with ^{177}Lu-DOTATATE treatment [55, 101, 102, 104]. Renal toxicity grade 4−5 was reported in 9.2% of the patients in a large phase II study in which 1109 patients diagnosed with NETs received ^{90}Y-DOTATOC [104]. However, two studies that reported greater yearly loss in renal function for ^{90}Y-, than for ^{177}Lu-DOTATATE reported lower mean absorbed doses after ^{177}Lu therapy, which means that the therapies are not directly comparable [101, 102]. The higher energy and longer range of β-emission from ^{90}Y compared to ^{177}Lu results in higher absorbed doses to the kidneys for the same administered activity, and the dose delivery pattern varies [102].

1.6.2 Bone marrow exposure and haematological toxicity

The bone marrow is exposed during systemic radionuclide therapy as the radiopharmaceutical circulates throughout the body. If there was specific uptake of ^{177}Lu in the bone marrow, the exposure would be enhanced; however, this has not been reported in ^{177}Lu-DOTATATE treatment [69]. A dose limit of 2 Gy for the bone marrow is typically used [54], a value that originally comes from organ tolerance studies that used ^{131}I to treat thyroid cancer [105-107]. The limit is seldom reached in ^{177}Lu-DOTATATE treatment, as reported by studies that performed bone marrow dosimetry

(Table 1). The lower exposure, and the fact that a clear dose-response relationship not has been observed, explains why bone marrow dosimetry is not always reported. Instead, haematological toxicity as estimated by changes in haemoglobin (Hb), white blood cell (WBC) and platelet (PLT) counts, serves as a surrogate of bone marrow exposure.

Haematological toxicity is often observed during treatment, but it is usually mild and transient [55, 108]. However, more serious haematological toxicity (grade 3−4, NCI CTCAE) is reported in 3−10% of patients receiving ^{177}Lu-DOTATATE, and it can become dose-limiting [55, 56, 108]. The time it takes for Hb, WBC and PLT counts to return to baseline values is reported to be between 11 and 24 months [56, 61, 87]. Exposing the bone marrow to radiation also involves a risk of long-term effects, with myelodysplastic syndrome and leukaemia being reported in 1−2% of patients [54-56]. Other factors that affect the development of haematological toxicity include haematological baseline parameters, renal function, tumour burden and patient age [56, 108].

1.7 Biological response to ^{177}Lu-DOTATATE

Several strategies have been evaluated for measuring the effect of ^{177}Lu-DOTATATE treatment. These focus on the normal tissue response or on the tumour tissue response to exposure. Two clinical studies quantified double-strand breaks (DSBs) in peripheral blood lymphocytes after ^{177}Lu-DOTATATE treatment by quantifying γH2AX-foci, and both found correlations between the absorbed bone marrow dose and the development of DSB [109, 110]. The analysis of radiation-induced DNA damage to determine the individual radiosensitivity is being evaluated for external radiotherapy [111]. The dose-rates and fractionation will be quite different from internal radiotherapy though. Studying the magnitude and the duration of DSBs after irradiation may be relevant to both the normal tissue response and to the tumour response. A preclinical study of α-emitting ^{225}Ac-based, and ^{177}Lu-based PRRT, showed a correlation between the amount of radiopharmaceutical that was given and γH2AX-foci as well as tumour growth inhibition in mouse tumour cells [112].

A newer concept to evaluate respons to treatment is to analyse changes in disease specific gene transcripts in blood. NETest® is a PCR-based analysis of 51 NET-associated genes, and changes in the transcript profile is reported to have delineated surgical cytoreduction [113] as well as treatment response from ^{177}Lu-DOTATATE [114]. It was also observed that this test could predict response to somatostatin analogue treatment using octreotide [115].

1.8 Optimisation of ^{177}Lu-DOTATATE treatment

Different approaches with the aim to optimise ^{177}Lu-DOTATATE treatment are described. Better treatment efficacy is observed for patients with high tumour uptake [54], which is thought to be due to a higher density of SSTRs on the tumour cells. Accordingly, strategies that enhance ^{177}Lu-DOTATATE uptake have been explored. Pre-clinical studies on rodents showed upregulation of SSTR expression on tumour cells 4 to 40 days after administration of sub-optimal amounts of ^{177}Lu-DOTATATE [116-118], but no clinical studies have been reported.

It is assumed, that radiopharmaceutical internalisation, which is achieved using the somatostatin agonist octreotate, is a prerequisite for absorption of a sufficiently high dose and to elicit a response to treatment. However, recent pre-clinical and clinical studies of the somatostatin antagonist JR11 (^{177}Lu-DOTA-JR11) have shown higher absorbed tumour doses compared to ^{177}Lu-DOTATATE, even though a majority of the radiopharmaceutical was membrane-bound rather than internalised [119, 120].

Methods that protect the kidney and that minimise renal exposure have been investigated so that higher total amounts of ^{177}Lu-DOTATATE can be used [121]. Gelofusine, a plasma expander, inhibits renal ^{111}In-DTPA-octreotide uptake in humans, similar to the effects of positively-charged amino acids [122], and this compound is used as an alternative in some centres. Pre-clinical studies on the combination of the positively charged amino acid lysine and Gelofusine have been encouraging in terms of showing an additive protective effect [123], but comparative clinical studies are missing. Co-infusion of a scavenger with ^{177}Lu-DOTATATE may also be useful, to minimise the radiation effects. The endogenous scavenger α1-microglobulin (A1M) protected cells in culture from α-particle-induced radiation damage [124], and in a recent study on A1M labeled to ^{125}I, it was distributed in proximal tubules of mouse kidneys together with co-infused ^{111}In-octreotide [125]. It remains to be investigated if the effect is similar in humans, and if the tumour uptake and response is affected.

The amount of peptide added to ^{177}Lu needs to be high enough to avoid free ^{177}Lu to be administered, but to high amount of peptide on the other hand may involve saturation of the SSRTs and lower activity will be delivered. A study on pre-therapeutic ^{68}Ga-DOTATOC and subsequent therapeutic ^{177}Lu-DOTATATE uptake, found that normal tissue SSTRs got saturated while tumour uptake not was affected [126]. This implies that normal tissue may be

protected by peptide delivered at therapy or before, and this would enable higher amounts of ^{177}Lu-DOTATATE to be given without increasing the normal tissue exposure. Individual studies are needed to evaluate when SSTRs on the tumour are saturated though. In contrast to these findings, Velikyan et al. observed decreasing tumour-to-normal tissue ratios as the increasing amounts of octreotide was administered at ^{68}Ga-DOTATOC diagnostics [127].

NETs can besides SSTRs also express receptors for glucagon-like peptide 1, cholecystokinin, and gastrin-releasing peptide for example, and peptide analogues to target these are being investigated [128]. Glucagon-like peptide 1-receptors is overexpressed in insulinomas, and sometimes in gastinomas and pheocromocytomas. Targeting of this receptor is being evaluated clinically in localisation studies with ^{111}In-DOTA-exendin-4 [129] and preclinically in organ distribution studies with ^{177}Lu-labeled exendin-4 [130]. Its safety and potential as a therapeutic agent needs to be further investigated.

2 AIM

The aim of the studies included in this thesis was to analyse normal tissue response in PRRT with a focus on ^{177}Lu-DOTATATE, for improved understanding of this therapy and better prerequisites for treatment optimisation in the future.

2.1 Pre-clinical study

The pre-clinical study (Paper I) explored renal toxicity in nude mice by examining biochemistry and morphology after distribution of high amounts of ^{177}Lu-, or ^{90}Y-DOTATATE. The aim was to evaluate if selective, and differential morphological changes in renal cortex would be possible to quantify. This as the uptake is known to be inhomogeneous and different, since the two radiopharmaceuticals have different physical properties.

2.2 Clinical studies

The objectives of the clinical studies (Paper II, III and IV) were to evaluate normal tissue response in the two major dose-limiting organs in SSTR-based PRRT; the kidneys and the bone marrow, and also the spleen.

The specific aims of the three clinical studies are summarized as:

- To analyse what impact renal function has on renal absorbed dose and the development of haematological toxicity (II)
- To develop a novel image-based method for bone marrow dosimetry in ^{177}Lu-DOTATATE treatment and investigate the correlation to haematological toxicity (III)
- To examine the role of the spleen for the development of haematological toxicity in ^{177}Lu-DOTATATE treatment (IV)

3 SUBJECTS AND METHODS

3.1 Pre-clinical study (I)

For the pre-clinical study of renal toxicity following ^{177}Lu-DOTATATE, nude female BALB/c mice were used. These mice were chosen due to the long experience of this animal model by the research group. The inherited immunodeficiency was not expected to affect the results. The experiments were approved by the Ethical Committee for Animal Research at Göteborg University and all animal procedures were consistent with the animal use guidelines of the United Kingdom coordinating committee on Cancer Research.

The animals (n=7–8 in each group) received varying amounts of ^{177}Lu-, or ^{90}Y-DOTATATE at 5 weeks of age. The radiopharmaceutical was administered as a single bolus subcutaneous injection. The amount of activity was chosen to be therapeutic and to cause measurable renal damage from what had been observed in earlier studies [116]. The mice receiving ^{177}Lu-DOTATATE were divided into groups injected with 90, 120, or 150 MBq, and the mice receiving ^{90}Y-DOTATATE were divided into groups injected with 10, 20, or 30 MBq.

To follow the general condition of the animals, body weight was measured once a week throughout the trial period, and signs of bone marrow toxicity was monitored by blood sampling once or twice a week the first month after injection, and then at sacrifice 6 months later. During the six months of follow-up, blood samples were collected from the tail vein. For long-term follow-up, blood samples were collected by heart puncture at the time of sacrifice. Haemoglobin (Hb), white blood cell (WBC) and platelet (PLT) counts were analysed using a cell counter. To explore long-term renal toxicity; creatinine, cystatin C and urea in serum was analysed by standardised clinical chemistry analyses at the time of sacrifice.

Morphological changes in the renal cortex were examined in tissue sections prepared from paraffin-embedded renal tissues (4 μm) and stained by periodic acid Schiff (PAS), haematoxylin–eosin, silver methenamine, or Van Gieson. To evaluate quantitative changes in renal cortex, the relative areas occupied by the different subunits (glomeruli, proximal tubules, and distal tubules) were calculated using point counting. This method includes placing a standard grid, containing a large number of points, on a photographed cross-section of the renal cortex. The number of points, which coincide with

the subunit, in comparison with the total number of grid points, gives the surface proportion of the subunit [131]. The qualitative morphological changes observed in the renal cortex were analysed by a pathologist.

3.1.1 Dosimetry

The radiopharmaceutical is reabsorbed and retained in the proximal tubules, situated in the cortex of the kidneys. Due to the small dimensions, part of the emitted energy will be deposited outside the renal cortex. To estimate the absorbed dose distribution in the mouse kidney, detailed Monte Carlo calculations were performed using MCNP5 (Los Alamos National LAB, NM, USA). The structure of the kidneys was determined using tissue sections prepared from paraffin-embedded kidney tissues (4 μm). The kidney was divided into three regions; inner and outer medulla, and cortex as shown in Figure 1. These regions were modelled as prolate spheroids in the MCNP5 program, and dimensions for an estimated kidney weight at time of injection (0.15 g) or at sacrifice (0.20 g) were used, with a tissue density of 1.03 g/cm3 [132]. The activity source was placed in the different regions, and absorbed fractions for the emitted radiation from ^{177}Lu and ^{90}Y were simulated, and the S-values calculated. The decay data for the radionuclides were taken from the MIRD decay scheme database [133]. The mean absorbed dose calculations for the kidneys were then based on the absorbed fractions determined above, and previously calculated kinetic data for ^{177}Lu-DOTATATE [134].

To compare absorbed doses with different patterns of delivery according to fractionation, dose-rate and radiosensitivity, the term biologically effective dose (BED) is useful. The BED is described in the context of the linear–quadratic (LQ) model, originally developed for external radiation therapy, but later revised for targeted radiotherapy such as PRRT by Dale [100]. When only one fraction/injection of activity is administrated the formula for BED will be:

$$BED = D + \beta/\alpha \cdot \frac{T_{1/2rep}}{(T_{1/2rep}+T_{1/2eff})} \cdot D^2 \qquad \text{(Eq. 3)}$$

Here, D is the cortex dose; β/α is the radiosensitivity parameter and was set to 0.38; $T_{1/2rep}$ is the repair half-time for the kidneys and was set to 2.8 h; and $T_{1/2eff}$ is the effective half-life of the radiopharmaceutical in the kidneys and was determined to be 49 h [134].

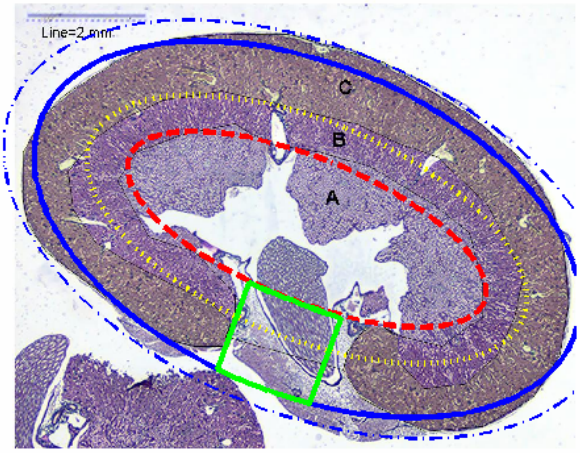

Figure 1. A mouse kidney divided into three regions for dosimetry: (A) inner medulla, (B) outer medulla, and (C) cortex. The outer boundary for a 0.15 g kidney is depicted by a blue continuous line and for a 0.20 g kidney by a blue dash-dotted line. The green box indicates the pelvis of the kidney.

3.2 Clinical studies (II, III, IV)

In the clinical studies, 51 consecutive patients with NETs, who received ^{177}Lu-DOTATATE at Sahlgrenska University Hospital between 2006 and 2011, were evaluated. These retrospective studies were approved by the Regional Ethics Review Board in Gothenburg and performed in accordance with the principles of the Declaration of Helsinki and national regulations. Patient characteristics are shown in Table 2.

Table 2. Patient characteristics according to gender, primary tumour origin, metastatic organs and previous treatment

Characteristic	Patients, n
Gender	
Male	31
Female	20
Primary tumour origin	
Small intestine	30
Pancreas	11
Rectum	4
Other	6
Metastatic organ	
Liver	36
Lymph nodes/soft tissue	33
Bone	18
Other	6
Previous treatment	
Hepatic artery embolization	16
Chemotherapy	15
External beam radiation	3
Liver transplantation	4

Patients included in the studies were judged to have tumours overexpressing SSTRs by a tumour uptake exceeding physiological liver-uptake on SSTR scintigraphy (Octreoscan®). The requirement to have tumours overexpressing SSTRs comes from experiences from Krenning et al. [60]. In their study on 131 patients receiving ^{177}Lu-DOTATE, high uptake on SSTR scintigraphy was correlated to higher remission rates.

All patients had progressive disease clinically, biochemically or radiologically at start. Treatment was given as a 30 minute-infusion of 7.5 GBq (3.5−8.3 GBq) of ^{177}Lu-DOTATATE on one to six occasions, at intervals of approximately eight weeks. Kidney protecting amino acids (lys/arg 2.5% in 1 l of 0.9% NaCl, infusion rate 250 ml/h) were co-infused with the radiopharmaceutical. As antiemetic prophylaxis, granisetron (3 mg) and betamethasone (4 mg) were administered. Patients stayed over night.

Patients were followed according to tolerance clinically and by blood sampling for Hb, WBC and PLT counts, and creatinine in serum every other week during the treatment period.

3.2.1 Dosimetry

Image acquisition

For dosimetry purposes, anterior and posterior planar gamma camera images were acquired at 2, 24, 48, and 168 h post-injection (p.i.). This was complemented with a single photon emission computed tomography and a low resolution CT (SPECT/CT) at 24 h p.i.

The effective attenuation coefficient and sensitivity for the gamma cameras were determined by planar scintigraphy of a planar ^{177}Lu-source equal to the cross area of a standard kidney, placed at different depths in a phantom of tissue equivalent material. In the planar images, the number of counts in a region of interest (ROI) drawn around the ^{177}Lu source was registered. A monoexponential curve was fitted to the number of counts versus depth data, and the effective attenuation coefficient and the sensitivity was determined.

Kidney and spleen dosimetry

For kidney and spleen dosimetry, thickness of the body over the organs and organ thickness were determined from a low-resolution CT performed at 24 h p.i. The number of counts in the anterior and posterior images was registered in a ROI around the organ and subtracted by the counts from a background ROI located caudal to the organ ROI.

The effective attenuation coefficient, sensitivity, anterior and posterior counts, patient thickness, and organ thickness were inserted into the conjugate view formula (Eq. 1) to obtain the activity for the different time points. A combined linear and monoexponential curve fit was applied to the time-activity data and the accumulated activity calculated. Kidney dosimetry was performed using the activity data from the 2D images, while spleen dosimetry was performed as a hybrid method, where the time-activity curve was adjusted after quantification of the activity in the spleen in the 24 h SPECT/CT. The measured activity in the spleen was adjusted to compensate for the partial volume effect (PVE). For this adjustment a correction factor was decided experimentally by placing activity in the spleen in the CT image and performing Monte-Carlo simulations utilising the medical physics, oncology, and nuclear medicine image research platform at Sahlgrenska Academy (PhONSAi; [135]).

The mean absorbed dose was estimated by assuming local absorption of the charged particles emitted from ^{177}Lu and neglecting the minor contribution from photons (≤2%; [50, 66]). The organ mass was estimated from the images of a high resolution CT performed before treatment.

Bone marrow dosimetry

The method developed for bone marrow dosimetry was based on a two-compartment approach that separates the high uptake area from the low uptake area in geometric mean images produced from the anterior and posterior whole-body images, as illustrated in Figure 2. An automated algorithm is utilised for the compartment separation, to avoid operator dependence. A whole-body ROI was created, and the pixel counts in this ROI were thresholded between 0 and the maximum pixel value. At each threshold value, a connected-component labelling algorithm was used to outline separate uptake foci in the whole-body image. The number of uptake foci (NUF) was calculated at each threshold value, generating a distribution of NUF versus a threshold index (ThI) defined as:

$$ThI = \frac{c_{max} - c_{thr}}{c_{max}} \qquad \text{(Eq. 4)}$$

Here, c_{max} is the maximum pixel value in the whole-body ROI and c_{thr} is the pixel threshold value. The NUF was normalised (nNUF) to the maximum number of uptake foci and could then be described as a function of ThI, ranging from 0 to 1. The algorithm was implemented into the image-platform PhONSAi. The distribution of nNUF versus ThI was analysed for all images to define an appropriate nNUF threshold value that separates the whole-body into high and low uptake compartments. The defined nNUF threshold value was applied to all time points and all patients.

The high uptake compartment includes organs with physiologically or pathologically high SSTR expression, such as the liver, spleen, kidneys, and tumours, and the low-uptake compartment corresponds to the remainder of the body.

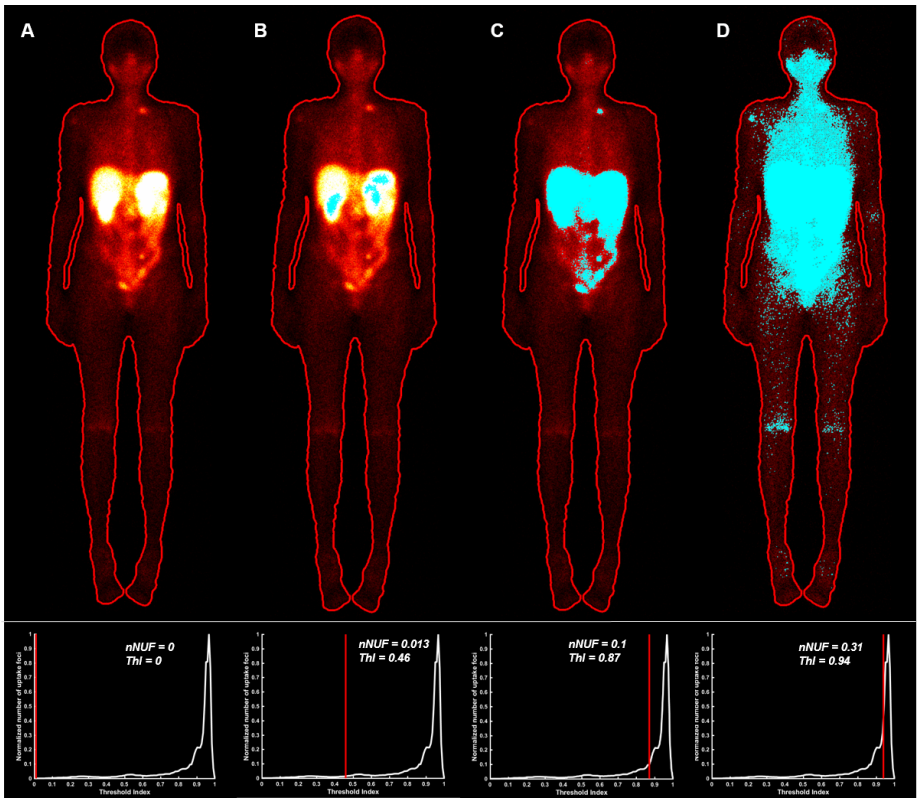

Figure 2. (A) A region of interest of the whole-body. (B) The automated segmentation tool has started to include foci in the whole-body starting with the highest uptake foci to the left on the x-axis. (C) Moving to the right, more and more foci will be included until a threshold is reached, where the number of foci increases instantly (D). The cut-off between the high and low uptake compartments (nNUF = 0.1) is set at the threshold value illustrated in (C). nNUF = normalized number of uptake foci. ThI = threshold index.

The activity in the two compartments was quantified according to the conjugate view method and time-activity curves created. For the conjugate view calculations, the patient-specific thickness of the high uptake compartment was determined over the abdomen from CT images and the activity assumed to be concentrated to a volume with a general organ thickness determined from a series of measurements in SPECT images (8 cm). The weight of the high uptake compartment was determined by assuming a density of unity and calculating the volume from the abdominal thickness and the area of the high uptake compartment. The thickness of the low uptake compartment was determined as the patient-specific weight minus

the calculated weight of the high uptake compartment divided by the area of the low uptake compartment. The accumulated activity in the under-, and overlying tissue of the high uptake compartment was added to the low uptake compartment.

The time-activity curves were fitted to a biexponential function for the low uptake compartment and to a combined linear and monoexponential function for the high uptake compartment, and the accumulated activity was then determined by calculating the area under the curve.

The activity in the low uptake compartment and its kinetics was utilised as an indirect measurement of the activity in the bone marrow. To investigate the relationship between the activity concentration in the bone marrow and the calculated activity concentration in the low uptake compartment, measurements in the SPECT/CT were performed. The low uptake compartment was considered to consist mainly of muscle, fat, and bone. A volume of interest (VOI) was applied in the centre of a lumbar vertebra (L4) to represent the bone marrow, and another VOI was symmetrically applied around L4 to represent the low uptake compartment, as shown in Figure 3. The ratio between the activity concentrations in these two VOIs was determined from 53 SPECT/CT images from 15 patients without known tumour infiltration in the bone marrow or the tissue surrounding the VOI. The measured activity in the bone marrow VOI was corrected for the partial volume effect, decided as described above. The ratio was assumed to be constant over time. L4 was chosen because the bone marrow volume could be delineated in the CT due to its size and horizontal orientation.

The mean absorbed dose to the bone marrow (D_{bm}) was calculated as the sum of the self-dose from the charged particles in the bone marrow itself and the cross-doses (γ-radiation) from the high and low uptake compartments using the equation:

$$D_{bm} = \tilde{A}_{bm} \cdot S_{bm \leftarrow bm} + \tilde{A}_{high} \cdot S_{bm \leftarrow high} + \tilde{A}_{low} \cdot S_{bm \leftarrow low} \qquad \text{(Eq. 5)}$$

Here, the accumulated activity in the bone marrow ($\tilde{A}_{bm}$) was derived from the accumulated activity in the low uptake compartment ($\tilde{A}_{low}$) and adjusted by the calculated ratio of the activity concentrations in the bone marrow and the low uptake compartment. The S-values were obtained from the specific absorbed fractions defined on the RADAR website [136]. The S-value for the γ-contribution from the high uptake compartment was calculated as a weight-weighted mean of the S-values for liver, spleen, and kidneys ($S_{bm \leftarrow high}$), and

from the low uptake area as a mean of the S-values for muscle and bone ($S_{bm \leftarrow low}$).

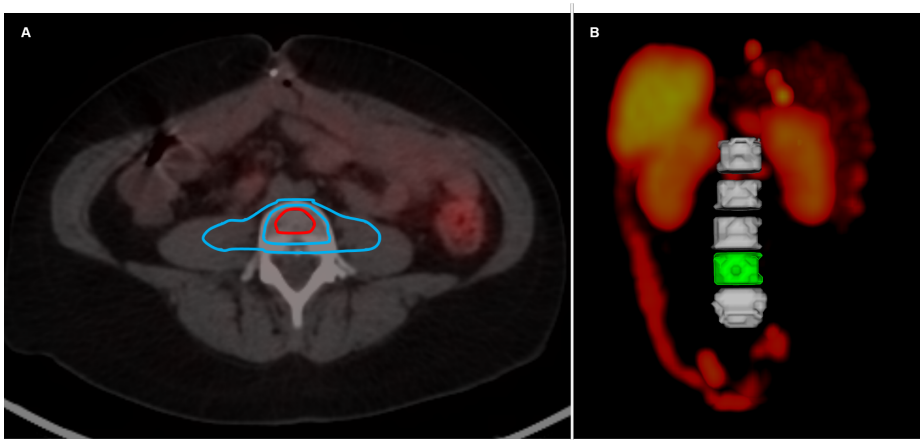

Figure 3. (A) Cross-section of an abdominal CT scan with a delineated volume of interest (VOI) around the bone marrow in the lumbar spine (L4) and a surrounding VOI representing the low uptake compartment in the whole-body. (B) Posterior view of a SPECT scan illustrating the localization of lumbar spines L1-L5 (L4 green) and their relation to abdominal organs. A physiological uptake in the kidneys and in the spleen can be observed, and a pathological uptake in multiple tumours in the liver.

3.2.2 Whole-body residence time

The conjugate view method was applied to estimate the whole-body residence time for ^{177}Lu. The patient thickness in the conjugate view formula was based on the thickness over the kidneys, but adjusted since it was notified that the activity otherwise would be underestimated. The adjustment was based on the activity data obtained from patients that had not urinated before the first image acquisition.

3.2.3 Tumour burden

Tumour burden was visually estimated for all patients. It was graded from 1 (minor tumour burden) to 5 (major tumour burden) in the planar image obtained 24 h p.i. at the first fraction. For comparative analysis, patients graded 1 or 2 were considered to have a small tumour burden, if graded 3 a medium tumour burden, and patients graded 4 or 5 were considered to have a large tumour burden (Figure 4).

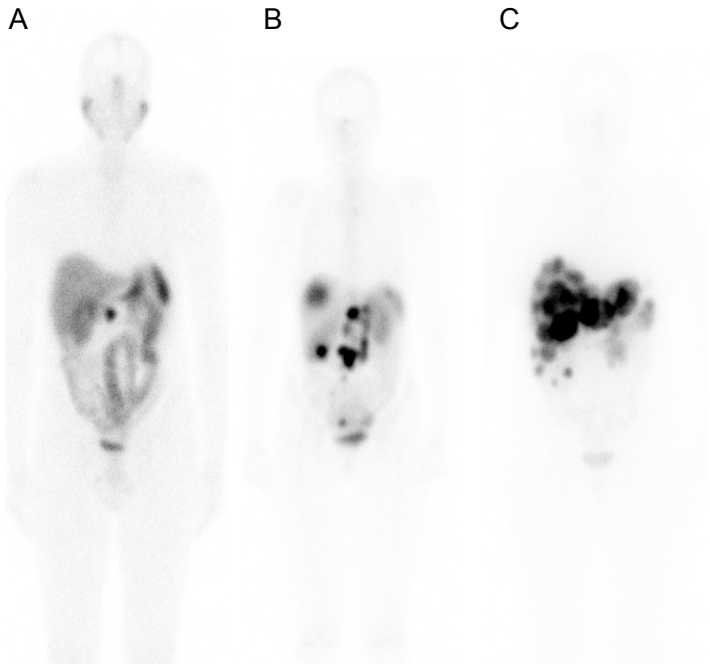

Figure 4. Examples of patients with different tumour burden. (A) A patient with a single tumour in the abdomen (small tumour burden), (B) a patient with multiple tumours in the abdomen including the liver (medium tumour burden), and (C) a patient with multiple liver metastases involving close to 50 % of the parenchyma.

3.2.4 Spleen volume assessment

Diagnostic CT was used for the volume estimations of the spleen, before treatment an in long-term follow up by manual VOI drawing in the image platform PhONSAi.

4 RESULTS

4.1 Pre-clinical study (I)

The pre-clinical study evaluated acute and long-term toxicity in nude mice after distribution of high amounts of ^{177}Lu-DOTATATE (90, 120 or 150 MBq) or ^{90}Y-DOTATATE (10, 20 or 30 MBq).

Weight gain

The mice in all three groups injected with ^{177}Lu-DOTATATE, gained weight slower than the control group initially ($p<0.05$). The weight gain was 14±1.7% (90 MBq), 10±3.5% (120 MBq) and 9±2.7% (150 MBq) to be compared to 30±4.5% for the control animals during the first 4 weeks. However, during the remaining follow up no differences in weight gain was observed. The mice injected with ^{90}Y-DOTATATE experienced a dose-dependent weight loss during the first week. In the group receiving the highest amount of ^{90}Y (30 MBq) five animals were sacrificed during follow-up because of more than 10% weight loss.

Haematological toxicity

The animals injected with ^{177}Lu-DOTATATE experienced moderate haematological toxicity with a mean decline in WBC counts of 23±3% from baseline values 10 days p.i. for the animals receiving the highest amount. A more pronounced decline in WBC counts was seen in all groups injected with ^{90}Y-DOTATATE, with a medium decline of 50±4% from baseline values 10 days p.i. in the two groups receiving the highest amounts. All groups receiving ^{177}Lu-DOTATATE recovered and blood counts did not differ from baseline values at 6 months of follow-up. In contrast, all groups receiving ^{90}Y-DOTATATE experienced marked long-term haematological toxicity according to WBC counts, with a remaining decline of 20% (10 MBq) to 60% (30 MBq) from baseline values. Hb and PLT counts were only scarcely reduced. The pronounced weight loss in the group receiving the highest amount of ^{90}Y, and the subsequent need to sacrifice more than half of these animals, could be due to haematological toxicity.

Renal dosimetry

The dosimetric calculation was adjusted to the assumption that the activity was located in the cortex (region C in Figure 1) instead of being uniformely distributed in the whole kidney. This has been described in localisation studies of radiolabeled somatostatin analogues performed by Melis et al. [94, 137]. Two values for kidney weight were compared; 0.15 g and 0.20 g, the

lower weight being closer to the weight at time of the injection and the higher weight at time of sacrifice. Monte Carlo simulations of the S-values for different regions of activity are summarised in Table 3.

Table 3. S-values for ^{90}Y and ^{177}Lu, distributed in the renal cortex or in the whole kidney

	Absorbed dose rate per unit activity S(T←S) (mGy.MBq-1.s-1)							
	Source organ							
	Cortex		Whole kidney		Cortex		Whole kidney	
	(0.15 g kidney)		(0.15 g)		(0.20 g kidney)		(0.20 g)	
Target organ	^{90}Y	^{177}Lu	^{90}Y	^{177}Lu	^{90}Y	^{177}Lu	^{90}Y	^{177}Lu
Inner medulla	0.288	0.001	0.596	0.167	0.222	0.001	0.469	0.121
Outer medulla	0.358	0.035	0.538	0.166	0.280	0.024	0.425	0.121
Cortex	0.455	0.217	0.411	0.148	0.359	0.162	0.323	0.110
Renal pelvis	0.287	0.019	0.358	0.028	0.228	0.014	0.283	0.020
Total kidney	0.408	0.145	0.459	0.151	0.321	0.108	0.363	0.112

It was found that only a small fraction of the emitted energy from ^{90}Y was deposited in the renal cortex, whereas most of the energy from ^{177}Lu was deposited here (30% vs. 85%). It was not possible to compare the toxicity profiles of the renal cortex for equal mean absorbed doses of ^{177}Lu and ^{90}Y (90 MBq vs. 50 MBq) in this animal model as other toxicity became dose-limiting already for the animals receiving 30 MBq of ^{90}Y. The mean absorbed dose to renal cortex for the animals receiving ^{177}Lu were 35, 47 and 58 Gy respectively, compared to 18 Gy for the animals receiving the highest amount of ^{90}Y (30 MBq).

Biomarkers of renal function

Long-term renal toxicity for all groups receiving ^{177}Lu-DOTATATE was observed by persisting increased creatinine values in serum at time of sacrifice, as shown in Figure 5. The group injected with the highest amount of ^{177}Lu-DOTATATE also had increased urea levels indicating a more severe effect on renal function, while Cystatin C not was affected in any of the groups. No biochemical changes were observed for the animals receiving ^{90}Y-DOTATATE.

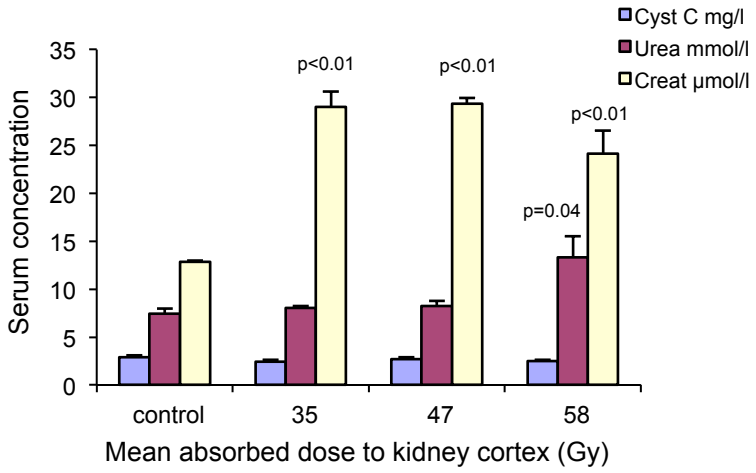

Figure 5. Biomarkers in serum 6 months after ^{177}Lu-DOTATATE injection indicated impaired renal function in all treated groups. Error bars describe the standard errors of the mean (SEM).

Renal morphology

Morphological changes in renal cortex were observed in all groups injected with ^{177}Lu-DOTATATE. For the group receiving the highest absorbed dose, 58 Gy, a severe loss of cortex parenchyma was observed; mainly due to a loss of proximal tubules, whereas distal tubules and glomeruli appeared to be preserved. The morphological changes in renal cortex were quantified applying the point-counting method to determine the relative area of the different subunits. This showed that an increasing number of proximal tubules were lost as the absorbed dose to renal cortex increased, whereas distal tubules and glomeruli were preserved, leading to a small increase of the relative area of these subunits at higher doses, as shown in Figure 6.

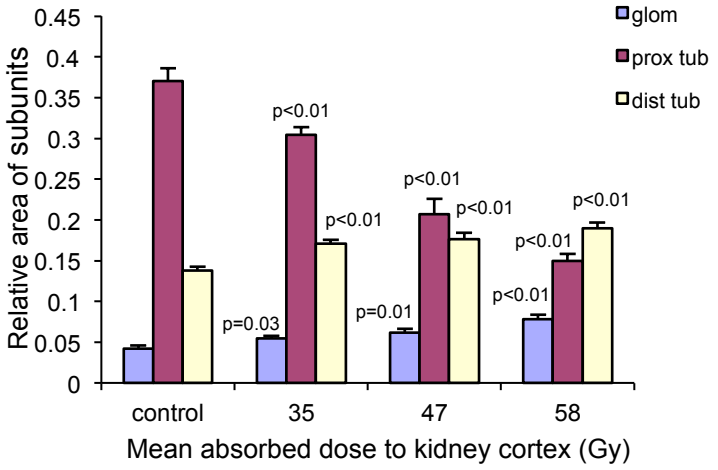

Figure 6. The relative area of proximal tubules declined with higher absorbed doses to renal cortex, whereas a small increase was seen for glomeruli and distal tubules. Error bars describe the standard errors of the mean (SEM).

The renal cortex was also evaluated for histological changes. In the proximal tubules; flattened epithelium, loss of brush border, dilatation, and empty lumina were observed 6 months after the ^{177}Lu-DOTATATE injection, as shown in Figure 7. No morphological changes were observed in distal tubules or glomeruli.

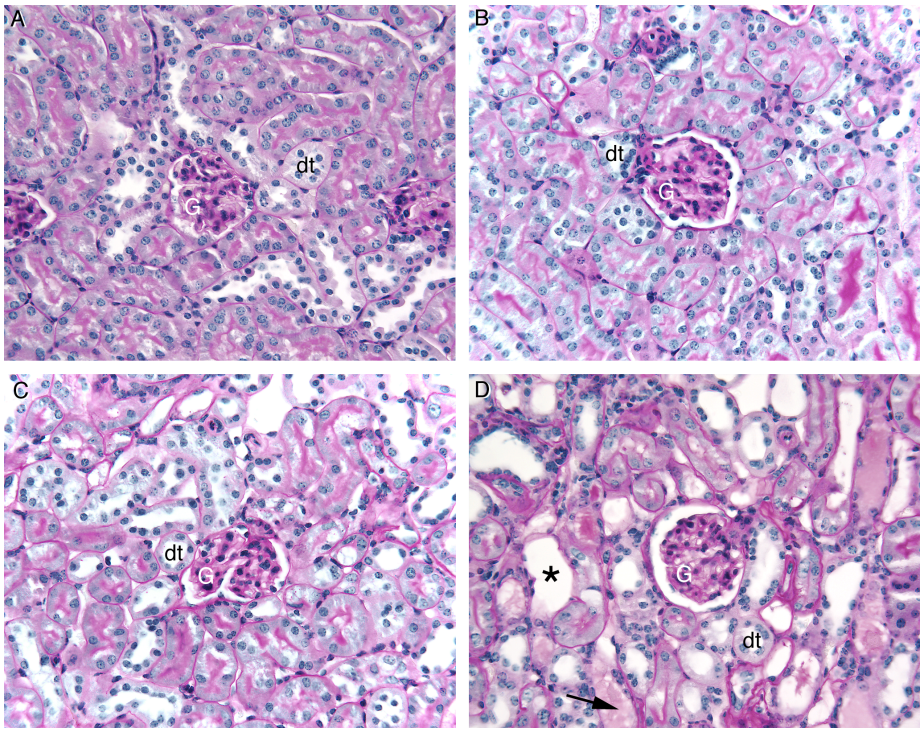

Figure 7. Morphological changes in renal cortex of nude mice after ^{177}Lu-DOTATATE injection. (A) Control tissue. (B) Cortex receiving 35 Gy or (C) 47 Gy exhibited smaller degenerative changes in proximal tubules with some loss of the brush border and slightly dilated lumina. (D) At 58 Gy proximal tubules were dilated and brush borders lost, resulting in empty looking lumina (star). Cellular debris, probably from necrotic cells (arrow), was observed. Glomeruli (G) and distal tubules (dt) remained intact.

Threshold dose values for proximal tubule damage

An estimation of a threshold value for detectable tissue damage after injection of ^{177}Lu-DOTATATE was done by a linear extrapolation of the relative area of proximal tubules vs. mean absorbed dose to renal cortex. The extrapolation of this line to the relative area of proximal tubules for the control animals resulted in a mean absorbed dose to cortex of 24 Gy, as shown in Figure 8 (threshold dose value). The mean absorbed dose to cortex for the animals receiving the highest amount of ^{90}Y-DOTATATE was 18 Gy, which is below the estimated threshold dose.

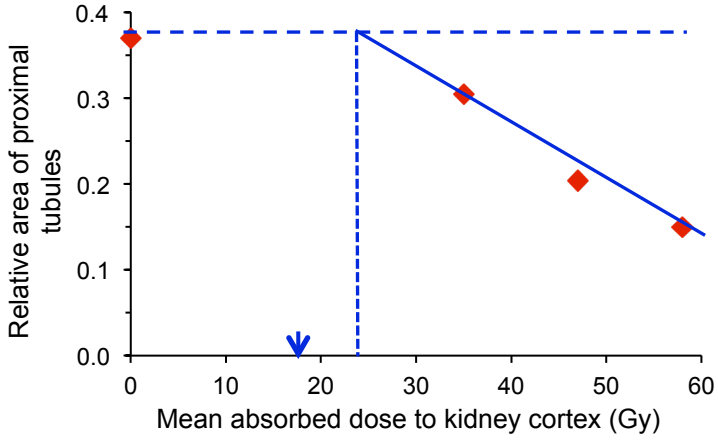

Figure 8. Relative area of proximal tubules vs. mean absorbed dose to renal cortex is illustrated. The red dots represent data for the three different mean absorbed doses to renal cortex from ^{177}Lu. The threshold dose value (24 Gy) for proximal tubule damage after injection of ^{177}Lu is indicated by a blue dotted line. The highest mean absorbed dose to renal cortex from ^{90}Y (18 Gy) is indicated by a blue arrow.

4.2 Clinical studies (II, III, IV)

The clinical studies evaluated different aspects of normal tissue response in ^{177}Lu-DOTATATE treatment, with focus on kidneys, bone marrow and the spleen. In paper III a novel image-based method for bone marrow dosimetry was developed.

It was found that patients with inferior renal function, estimated by GFR (^{51}Cr-EDTA-clearence) before treatment start, were exposed to significantly higher mean absorbed dose to the kidneys ($p<0.01$) during their first fraction of ^{177}Lu-DOTATATE (Figure 9). The variation was considerable, and more pronounced for patients with inferior renal function. Patients with GFR<60 ml/min (n=10, i.e. chronic kidney disease stage 1; [138]) received renal absorbed doses of 0.83±0.35 Gy/GBq as compared to 0.49±0.09 Gy/GBq for patients with GFR>90 ml/min (n=11, i.e. normal GFR for age-matched healthy persons; [139]).

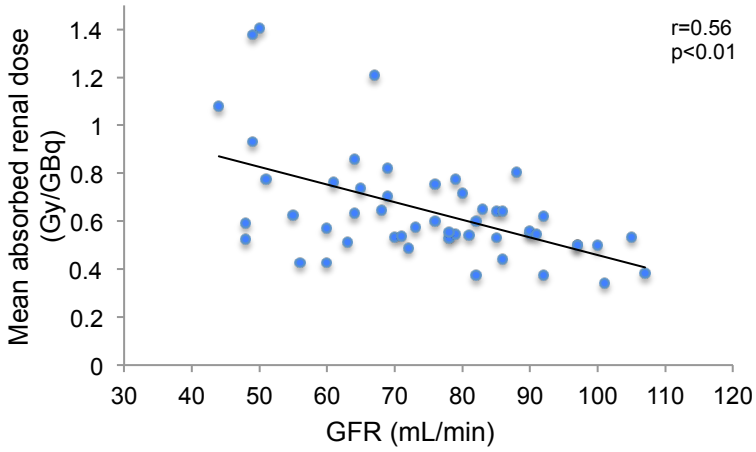

Figure 9. Patients with inferior renal function (GFR) were exposed to higher mean absorbed renal doses per injected amount of ^{177}Lu-DOTATATE.

Conditions known to influence renal function; including age, comorbidity (hypertension and diabetes mellitus), prior chemotherapy and nephrotoxic comedication, were analysed to evaluate their potential impact on radiation exposure of the kidneys. Renal function declines physiologically with age [140], and a trend toward this was observed among patients in this study, but the differences were not statistically significant. Baseline GFR was 65±16ml/min for patients older than 70 years (n=8) and 77±16ml/min for younger patients (n=43; p=0.07), and consequently the absorbed renal doses did not differ; 0.76±0.31 Gy/GBq compared to 0.62±0.20 Gy/GBq (p=0.12). When comparing patients with hypertension (n=15) or patients exposed to previous chemotherapy (n=15) to patients without these risk factors, no differences were observed either in baseline GFR or in absorbed renal dose. Patients with diabetes mellitus (n=2), and patients on comedication with a potential effect on renal function (n=2), were too few to analyse.

Renal function affected the development of haematological toxicity during treatment. GFR was 89±9 ml/min in patients who did not experience any haematological toxicity (Grade 0, NCI CTCAE) and 56±6 ml/min in those who developed the highest toxicity (Grade 3). These groups were small (three and four patients respectively), but their mean values differed significantly ($p<0.01$; Figure 10). Bone metastases are discussed as a risk factor for developing haematological toxicity, and in this study relevant haematological toxicity (Grade 2 or 3) was more frequent in patients with known bone

metastases (n=18); 61% compared to 43% of the other patients. No differences were seen according to the exposure to previous chemotherapy.

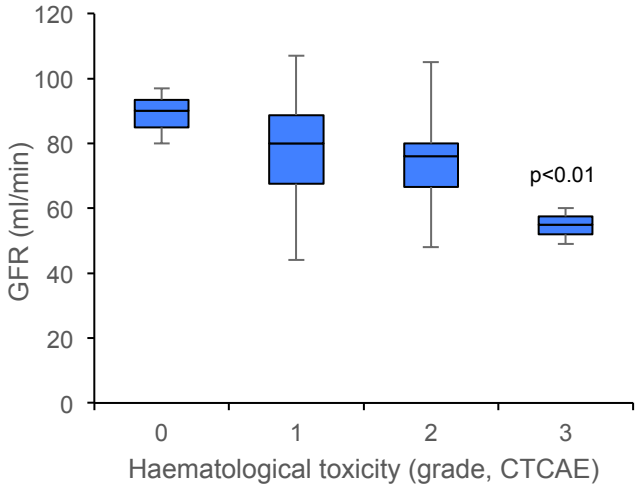

Figure 10. Patients with inferior renal function developed a higher grade of haematological toxicity during ^{177}Lu-DOTATATE treatment.

Tumour burden and whole-body residence time for ^{177}Lu was also analysed to evaluate their impact on normal tissue exposure. Renal function did not affect the residence time for ^{177}Lu in this study, and patients with longer residence time did not receive higher absorbed renal doses. However, the residence time did affect the development of haematological toxicity; it was estimated to 1.4±0.1 days for patients with no toxicity, compared to 2.3±0.5 days for patients who developed haematological toxicity grade 3 ($p<0.01$; Figure 11A). It was also observed that patients with larger tumour burden had a longer residence time compared to patients with smaller tumour burden (Figure 11B), and consequently the frequency of haematological toxicity grade 2-3 was higher (57% vs. 36%). Interestingly, patients with larger tumour burden did not receive higher absorbed renal doses, despite inferior renal function at treatment start; 72±14 ml/min compared to 84±11 ml/min ($p=0.02$).

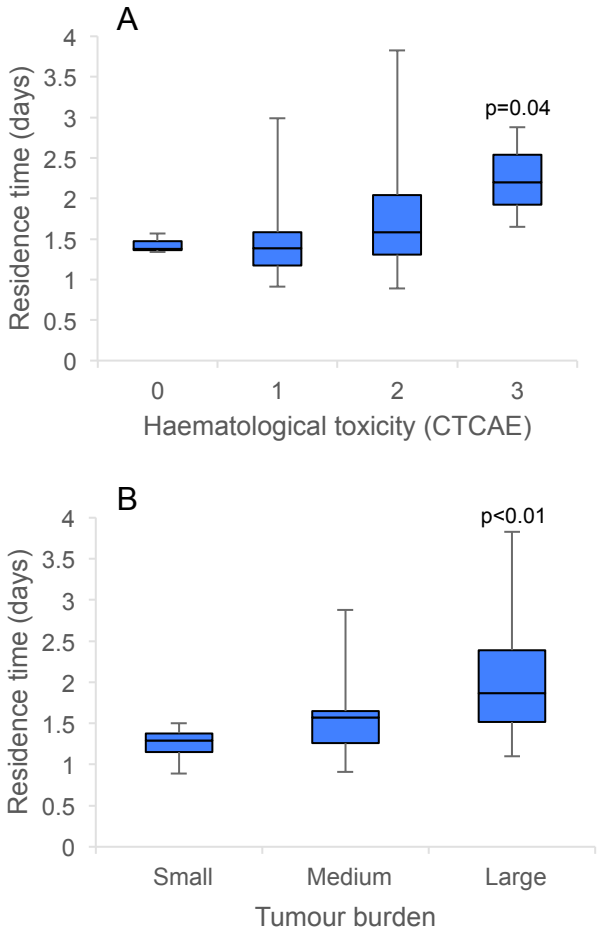

Figure 11. Longer whole-body residence time for ^{177}Lu was associated with (A) a higher grade of haematological toxicity and (B) a larger tumour burden.

The radiation exposure of the bone marrow was further analysed in paper III. A planar image-based method to estimate mean absorbed dose to the bone marrow was developed, and the association with haematological toxicity investigated.

The methodology for the planar dosimetry was used for all patients and possible to apply on all images. The automated segmentation tool used for analysis of the normalised numbers of uptake foci (nNUF) versus the

threshold index (ThI), showed a similar pattern in all images, as shown in Figure 2. The threshold value used to separate the high uptake compartment from the low uptake compartment was 0.1, implying that 10 % of the foci in the whole-body ROI was included in the high uptake compartment and 90% in the low uptake compartment.

After the compartment separation, the activity could be quantified for all time points. Time-activity curves were created and fitted to a biexponential function for the low uptake compartment for all fractions with 4 data-points (n=165), and to a monoexponential function if only 3 data-points could be acquired (n=9). For the high uptake compartment, time-activity curves were fitted to a combined linear and a monoexponential function. The effective half-lives for the first and second phases of the low uptake compartment were 2.4±1.7 h and 61±9 hours respectively. Most of the accumulated activity in the whole-body, 63±11%, was found to be located in the high uptake compartment, and 37±11% in the low uptake compartment.

The ratio between the activity concentration in the bone marrow and the low uptake compartment was found to be 1.8, when corrected for the partial volume effect. This factor was used to calculate the self-dose, which was added to the cross-doses from the high and low uptake compartments for the estimation of the bone marrow dose. The mean absorbed dose for the 46 patients included was 0.20±0.05 Gy per 7.4 GBq of ^{177}Lu-DOTATATE. The total absorbed dose was 0.64±0.22 Gy from an average amount of 24±7 GBq. The absorbed dose to the bone marrow was dominated by the self-dose**,** contributing to 85±4% of the total dose. The cross-doses from the high and the low uptake compartments contributed to 9±4 % and 6±2 % of the total dose, respectively.

Associations were found between absorbed bone marrow doses and developed haematological toxicity. The calculated mean absorbed dose per treatment, and also the total dose, correlated to the decrease in Hb, WBC and PLT counts (Figure 12).

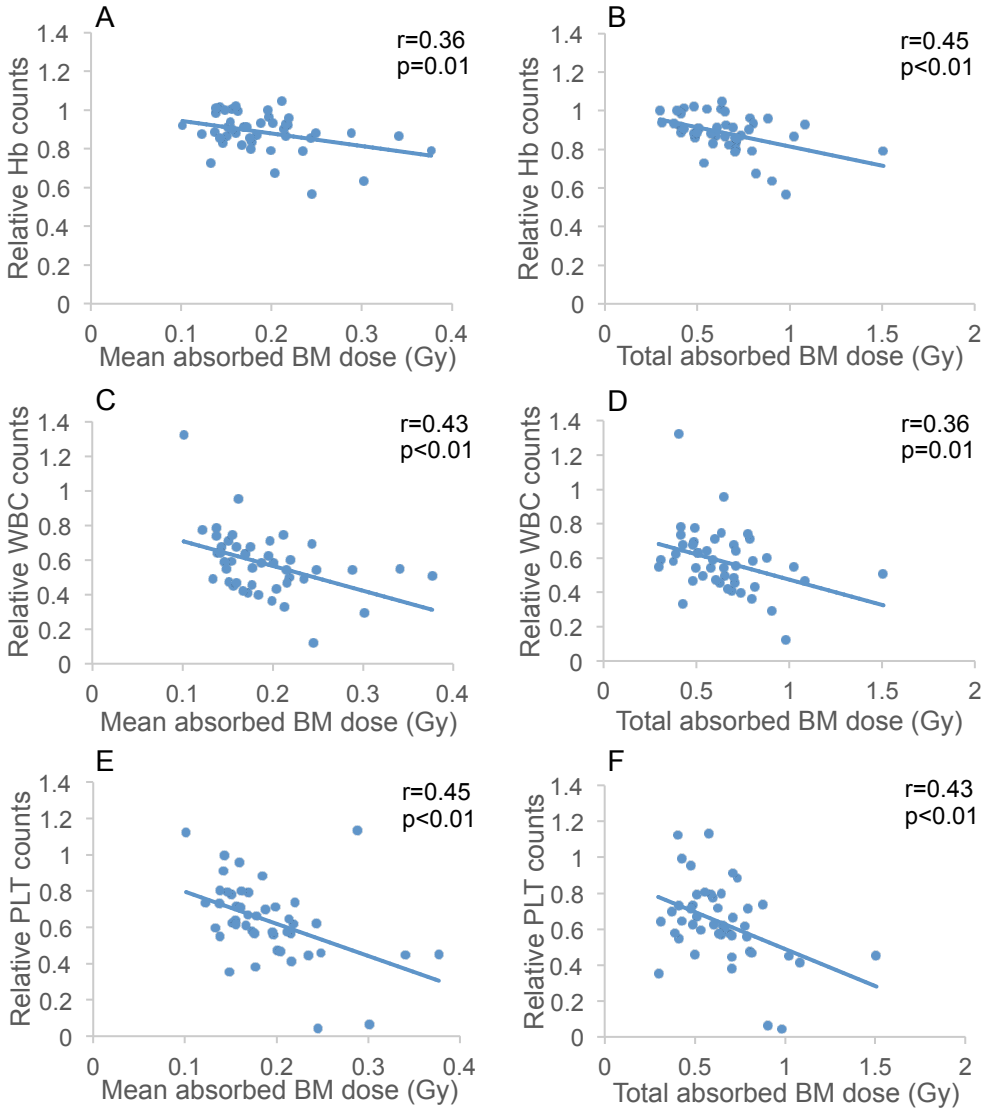

Figure 12. Correlations between mean and total absorbed bone marrow dose, and the decrease in Hb (A, B), WBC (C, D) and PLT (E, F) counts during ^{177}Lu-DOTATATE treatment. BM = bone marrow.

In general, a transient haematological response followed each fraction, and then Hb, WBC and PLT counts returned to baseline values, or close to baseline values, at the time of the next fraction given (Figure 13). All patients did however not respond in this predictive way. The lowest blood value measured during treatment was related to the absorbed dose, when exploring correlations.

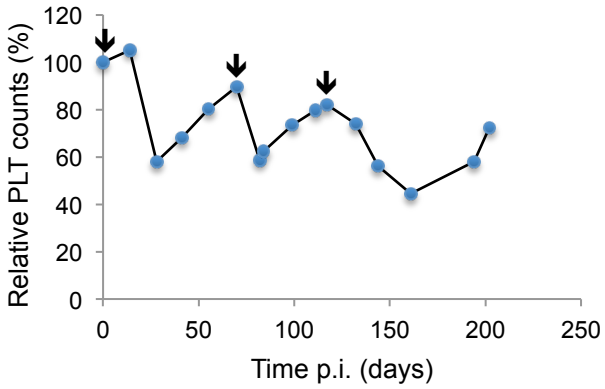

Figure 13. An example of PLT variation for a patient during three fractions of ^{177}Lu-DOTATATE. Arrows indicate the time point for each fraction. Blood sampling was performed every 2 weeks.

The radiation exposure of the spleen was investigated in Paper IV, as it may be relevant for the development of haematological toxicity. The uptake of the radiopharmaceutical in the spleen was relatively high. Mean absorbed dose to the spleen for the 41 patients included was 5.1±1.8 Gy per 7.4 GBq of ^{177}Lu-DOTATATE. Total absorbed dose was 17±6 Gy from an average amount of 24±7 GBq. The total absorbed spleen dose correlated to the decrease in Hb (p=0.02; Figure 14A**),** but not in WBC or PLT counts. A correlation was also observed between mean absorbed spleen dose and the decrease in PLT counts, although not significant (p=0.06; Figure 14C). This correlation reached significance for patients without bone metastases (n=26) (p=0.04; Figure 14D). Hb or WBC counts was not correlated with mean absorbed spleen dose.

The spleen showed a radiation response in terms of a volume reduction after ^{177}Lu-DOTATATE treatment. Mean volume of the spleen was 260 ml before treatment start to be compared with 200 ml at a mean follow-up of 36 months after the first fraction given; a decrease to 75±14 % of the original volume ($p<0.01$).

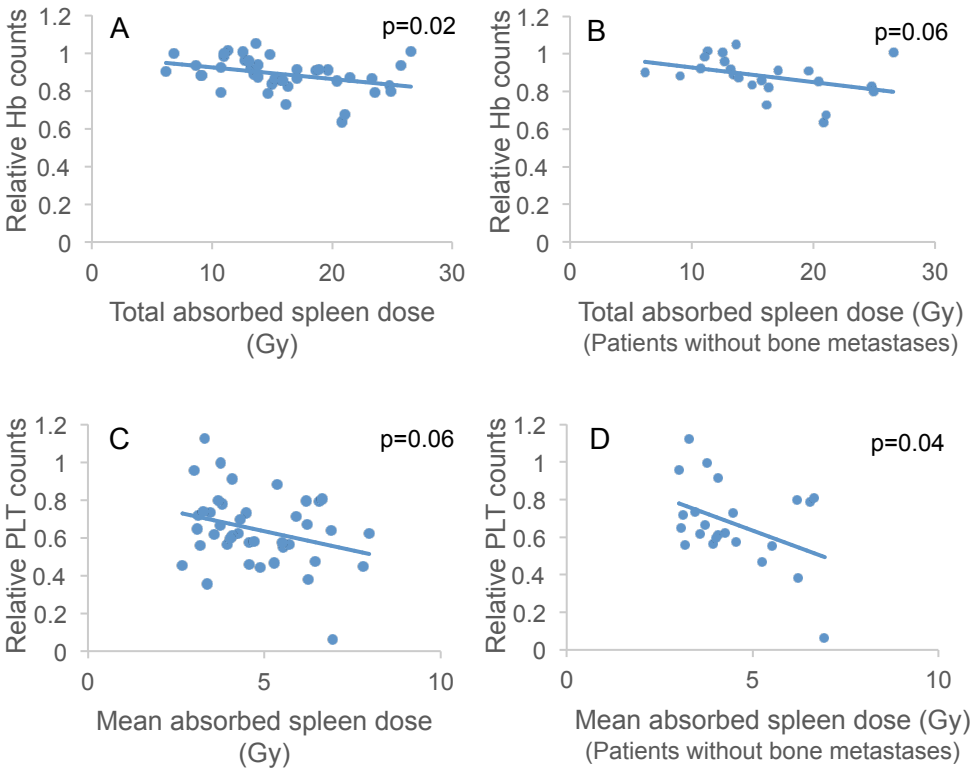

Figure 14. Correlations between total absorbed spleen dose and decrease in Hb counts, for all patients (A) and for patients without bone metastases (B), and correlations between mean absorbed spleen dose and decrease in PLT counts, for all patients (C) and for patients without bone metastases (D).

4.3 The combined effect of absorbed dose to bone marrow and spleen

Correlations between absorbed bone marrow dose (Paper III), and also absorbed spleen dose (Paper IV) and the haematological response were observed, although week. Further calculations from these results were made to investigate if bone marrow dose was stronger correlated to the haematological toxicity when the patient´s absorbed spleen dose also was included. In this complementary analysis 41 patients could be included. Here, a weighted spleen dose, D_{spleen}, was added to the absorbed bone marrow dose, $D_{BM,}$. The value for the weighting factor, ω, was chosen from were the optimal correlation to haematological toxicity was found (i.e. the highest value for Pearson´s R):

$$BRD = D_{BM} + \omega D_{Spleen} \qquad \text{(Eq. 6)}$$

The combined dose from bone marrow and spleen dose is named biological response dose *(BRD*) in the equation. The correlation between the combined dose, BRD (ω=0.013), and PLT counts, were stronger than for the bone marrow dose alone; r=0.59 and p=0.00005, compared to r=0.55 and p=0.0002. The correlation between the total absorbed dose to the bone marrow and Hb counts was also stronger when adding a weighted spleen dose to the bone marrow dose (ω=0.013; r=0.52 and p=0.0005 compared to r=0.49 and p=0.001).

5 DISCUSSION

5.1 Pre-clinical study (I)

In this study, it was found that high activities of ^{177}Lu-DOTATATE generated selective and dose-dependent morphological changes in renal cortex of nude mice. Elevated functional markers in serum also indicated renal toxicity. The selective damage to proximal tubules indicates an inhomogeneous dose distribution in cortex. More detailed dosimetric studies are needed to confirm this, however. No detectable morphological or biochemical changes were observed for the animals exposed to ^{90}Y-DOTATATE; probably due the low mean absorbed doses to renal cortex. At higher administered amounts of ^{90}Y-DOTATATE other toxicity became dose-limiting, detectable as haematological toxicity and weight loss. Liver toxicity, not monitored in this study, may also have contributed, but previous studies have estimated the liver dose to be very limited compared to the renal dose [134].

Serum creatinine was markedly elevated compared to baseline values (>100%) for all groups receiving ^{177}Lu-DOTATATE. The creatinine value was not further elevated, as the absorbed dose to the kidneys increased. This may be due to that creatinine not is reliable as the glomerular filtration rate becomes more affected, and tubular secretion becomes more important [141]. Increased urea values were observed only in the group receiving the highest mean absorbed dose, indicating more severe renal damage. Cystatin C, used as the third biochemical marker for renal function, seemed as a less sensitive marker for renal function in this study, as it did not increase from baseline values in any of the treated groups.

A threshold dose value of 24 Gy was estimated for detectable morphological changes in renal cortex. This value could not be verified for ^{177}Lu, as no animals were exposed to lower mean absorbed doses than 37 Gy. For the groups receiving ^{90}Y, mean absorbed doses were 18 Gy or less, and for these animals no morphological changes were observed. It should be noted that ^{177}Lu may not cause a similar pattern of damage as ^{90}Y at equivalent mean absorbed renal cortex doses, due to their different physical properties according to half-lives, and range of the emitted particles. The shorter range of electrons emitted from ^{177}Lu may cause more pronounced damage than ^{90}Y locally because very high absorbed doses are delivered to smaller areas with assumed high radiosensitivity. This was reflected in our study by selective morphological changes in proximal tubules, whereas the other subunits were

preserved. The reasons for the selective changes might be differences in the absorbed dose as well as in the radiosensitivity for the subunits. A more detailed dosimetric analysis of the mouse kidney to describe the dose distribution in cortex and the corresponding tissue response would enable an evaluation of the specific radiosensitivity of the different subunits. A detailed nephron-based model of the absorbed dose to the kidneys has been described by Hobbs et al. for α-emitters [142].

The amount of radiopharmaceutical given affects the time it takes to develop renal damage, and the severity of damage. In a study of rats injected with ^{177}Lu-DOTATATE, an earlier development of renal toxicity was observed at higher activities [143]. The mice injected with ^{90}Y in our study may have developed measurable renal damage if the follow-up had been extended. In the study on rats mentioned above, a more global damage in renal cortex was also observed as the amount of activity was increased, with morphological changes for distal tubules and glomeruli too.

Normal tissue response in mice from ^{177}Lu-DOTATATE treatment, does not immediately translate to normal tissue response in humans. There are important similarities; the uptake mechanism responsible for the tubule clearence of most proteins filtered in the glomeruli, the endocytic receptors megalin and cubulin on the proximal tubule cell, have been described both in humans and in rodents [93, 144]. Localisation studies have confirmed an inhomogeneous distribution of radioactivity in the kidneys for humans as well as for rodents, with the highest amount being present in the in the inner cortex and the outer medulla [94, 95], which would correspond to the location of proximal tubules in both species. However, several differences can be expected; in biodistribution of the radiopharmaceutical and in radiosensitivity. Furthermore, the human kidney is much larger than that of the mouse, which probably leads to more selective damage from ^{177}Lu in the human kidney and therefore other influences on renal function. Being aware of the different preconditions, it is interesting that the threshold dose values for mice in this study (24 Gy) are similar to the dose limits discussed and used for patients to avoid renal toxicity.

5.2 Clinical studies (II, III, IV)

Different aspects of normal tissue response during ^{177}Lu-DOTATATE treatment were evaluated. It was found that patients with inferior renal function were exposed to higher mean absorbed dose to the kidneys. There was however a considerable variation, and larger for patients in the lower range of glomerular filtration rate (GFR). Reasons for this variation are

probably both physical and biological. Variations are included in the 2D conjugate view method used. Most important of these is that the ROI drawn around the kidneys for activity quantification will include uptake in the tissues over-, or underlying the kidneys, such as the liver, intestine and tumours [66, 145]. 3D dosimetry utilising SPECT/CT imaging has prerequisites to be more accurate than 2D, but will require considerations of attenuation, scattering, resolution and partial volume effect [80, 146]. An alternative to the conjugate view method is quantification in the posterior planar image, with a ROI for background correction drawn around the whole kidney. This was shown to enhance the accuracy compared to activity concentration estimates performed with the conjugate view method [76].

The variations included in the method can however be expected to be independent of renal function. Therefore, the larger variation in patients with inferior renal function is probably due to biological phenomena. The renal function was estimated from the glomerular filtration rate by ^{51}Cr-EDTA-clearence, and the tubular function was not evaluated. Patients with lower GFR may differ in tubular function more markedly, which affects tubular reabsorption ability and exposure of the radiopharmaceutical from the primary urine. For a separate estimation of the tubular function, ^{99m}Tc-DMSA or ^{99m}Tc-MAG3 scintigraphy would have been accurate to perform [147-150], or urine sampling for a α1-microglobulin/creatinine ratio [151].

Hypertension and previous chemotherapy may have an impact on renal function and consequently on the radiation exposure of the kidneys. Guerriero et al. [152] observed significantly higher absorbed renal doses for patients with these two risk factors, in contrast to the findings in this study. They did not report renal function for the patients; in the present study patients with hypertension had a normal GFR. Patients treated with chemotherapy in this study also had a normal renal function as estimated by GFR at treatment start, even though a majority of the patients in the present study (13 of 15) had received streptozotocin or cisplatin, both known to cause renal toxicity. The time between completed chemotherapy and the start of ^{177}Lu-DOTATATE treatment was 9 months which may be considered a relatively long recovery time for normal tissues, including the kidneys.

Patients with inferior renal function also experienced a higher grade of haematological toxicity (according to NCI CTCAE), which is consistent with the findings from Bergsma et al. [108]. This may reflect that lower renal clearance affects the exposure of the bone marrow from the radiopharmaceutical. Impaired renal function may also influence the ability of erythropoietin production to stimulate erythrocyte regeneration [153].

Another condition that affects the exposure of the bone marrow is bone metastases. A higher frequency of haematological toxicity grade 2 to 3 was seen among these patients in the present study, just as Kam et al. have shown [154]. In contrast to what Kam found however, no differences in haematological toxicity was observed for patients exposed to chemotherapy. As mentioned above, the amount and type of chemotherapy might vary between studies, giving different preconditions for the viability of bone marrow.

For further evaluation of what decides the total radiation exposure and normal tissue response, the residence time of ^{177}Lu, and the tumour burden were analysed. The residence time was not affected by the renal function in this study, as opposed to what was expected. Besides the uncertainties in the method used, this indicates that other factors influence the residence time, such as the tumour burden. Higher tumour burden correlated to a longer residence time, and to a higher grade of haematological toxicity, in accordance to Bergsma´s study [108]. Interestingly, a longer residence time and a higher tumour burden did not affect the absorbed dose to the kidneys. The kidneys may be protected from radiation by the high tumour burden as a higher proportion of the radiopharmaceutical accumulates in the tumours. In a study by Garske et al. it was observed that renal doses increased as the tumour burden decreased, during repeated fractions of ^{177}Lu-DOTATATE [62, 155]. Patients with smaller tumour burden in the present study did not receive higher renal doses, however this may be due to a better renal function among these patients compared to patients with more extensive disease.

After the findings that residence time affected the haematological response, the bone marrow exposure was further evaluated in the following work. For a more detailed analysis of what affects the haematological toxicity, changes in absolute blood counts were used instead of graded toxicity (CTCAE) in paper III and IV. No clear correlations between mean absorbed bone marrow dose and haematological toxicity during ^{177}Lu-DOTATATE have been reported [66, 69]. This is probably due to that several factors have an impact on the haematological response, but also the fact that it is difficult to establish an accurate method for absorbed bone marrow dose estimates.

In Paper III, a novel image-based method for bone marrow dosimetry was developed. The obtained mean absorbed dose levels where comparable to earlier reported results for ^{177}Lu-DOTATATE, where blood-, urine- and image-based methods were applied [58, 61, 69, 156]. Furthermore, the mean absorbed dose to the bone marrow correlated with the haematological toxicity, though with large variations. The uncertainties depend, at least in

part, on the method used. The method for dividing the whole-body uptake into two compartments in an automated manner seemed applicable, but will share the uncertainties included in all planar dosimetry methods. Blood-based dosimetry on the other hand, will have uncertainties included in the timing and frequency of blood sampling, and in the activity quantification of the samples. Furthermore, the image-based method in the present study, just as blood-based methods, involves an indirect estimation of the activity concentration in the bone marrow, calculated by choosing a ratio between the compartment that is quantified and the bone marrow. In this study, the activity concentration in the centre of a lumbar vertebra, quantified in the SPECT 24 h p.i, represented the bone marrow. This will not take into account regional differences. The low uptake compartment was represented by the activity in a VOI drawn around the same vertebra, consisting mainly of muscle and bone. This is a simplification of the low uptake compartment, even though it is dominated by muscle, bone and fat tissue. The used ratio between the bone marrow and the low uptake compartment was calculated from patients without bone metastases, possibly underestimating the ratio for patients with bone metastases present. Mean absorbed bone marrow dose differed between these patients; 0.22 Gy for patients with bone metastases (n=18) compared to 0.18 Gy for the other patients (p=0.02). Differences in the kinetics between the two compartments may also exist. One study found an increase over time of the ratio between bone marrow and blood for patients treated with ^{131}I-based radioimmunotherapy [157]. This may have implications for PRRT to, though ^{131}I as compared to ^{177}Lu, and peptides as compared to antibodies, have different biodistributions.

Pure image-based methods to estimate the absorbed dose to the bone marrow in radionuclide therapy have been described previously, and originally for radioimmunotherapy, based on quantification of the accumulated activity in the sacral region in the post-therapeutic planar images [158]. Forrer et al. evaluated an image-based method to estimate the accumulated activity of ^{177}Lu-DOTATATE in the bone marrow by quantifying the activity concentration in the thoracic spine from SPECT images after therapy [69]. However, the authors concluded that the spine uptake was too close to background values. In a recent study, an image-based method for bone marrow dosimetry in ^{177}Lu-DOTATATE treatment was presented using repeated SPECT images for voxel-based quantification of the radioactivity in the lumbar spine, but the method was not verified against haematological toxicity [74]. Notably, the whole-body is normally not visualised with SPECT to avid too extensive acquisition times, and this will prevent whole-body dose estimates to be done.

Further optimisation of the developed method may show stronger correlations between mean absorbed bone marrow dose and haematological response. The S-values used were calculated from phantom-derived data published on the RADAR website [136]. Strategies for improvement of the method could include the finding of more patient specific S-values for cross-doses, and also the use of different scattering correction techniques and methodologies for attenuation correction, such as scout images.

The objective should be to make as accurate bone marrow dose estimates as possible, but it is clear that several other aspects will affect the haematological response. Earlier studies have shown associations to baseline values for WBCs, and age [56, 108]. A lower WBC count may reflect an already affected bone marrow, whereas higher age involves a physiological decline in bone marrow volume [159]. In paper II, correlations between haematological toxicity, and renal function, residence time and also tumour burden was observed, just as Bergsma has reported [108]. All these factors have prerequisites for increasing the bone marrow exposure. Sandström et al. observed that mean absorbed dose to the bone marrow declined with repeated fractions of ^{177}Lu-DOTATATE [58], possibly because of a descending tumour burden, and a consequent shorter residence time.

A potential protective effect according to developed haematological toxicity has been observed for splenectomy during ^{177}Lu-DOTATATE treatment [56]. The spleen, where blood cells are pooled, is often exposed to the highest mean absorbed dose [61], due to a high physiological uptake [92]. In paper IV, the radiation exposure of the spleen was explored, and a modest correlation was found between total absorbed dose to the spleen and the decrease in Hb counts. Mean absorbed dose to the spleen seemed correlated to the decrease in PLT counts, though it was only significant for patients without bone metastases. The reason for different haematological response according to the presence of bone metastases may reflect the heterogeneity of these patients.

In a study by Kulkarni et al., where 53 patients treated with ^{177}Lu-DOTATATE where included, no correlations between mean absorbed spleen dose and haematological toxicity was observed [160]. However these patients were evaluated after a mean absorbed spleen dose of 6 Gy, to be compared to 17 Gy in the present study, and the former may be too small an exposure for a detectable haematological response. Haematological toxicity is observed after external radiotherapy of the spleen, used in haematological disorders for pain relief, with the goal to diminish the dimensions of the spleen [161-163]. External radiotherapy described for haematological disorders was

fractionated 0.2-1 Gy to a total absorbed dose of 2-10 Gy. The haematological response to external radiotherapy already at low absorbed doses could be due to different properties of absorbed dose delivery according to fractionation size, dose rate and also according to radiosensitivity. Patients with haematological disorders generally have hematopoietic stem cells situated in the spleen, while patients in the present study probably have mainly mature blood cells situated here [164].

The spleen responded to radiation exposure from ^{177}Lu-DOTATATE with a reduction in volume, in accordance with what is observed from external radiotherapy [163, 165], despite different prerequisites according to fractionation, total dose, and splenic function.

After having evaluated correlations between absorbed bone marrow dose and also spleen dose, and developed haematological toxicity (Paper 3 and 4), a simple model was tested to find out if the correlation would be stronger if both these absorbed doses were taken into account. A modest positive effect on the association with the haematological response was achieved, which illustrates that the radiation exposure of both these organs should be evaluated, and a more accurate way to weigh them together would be of further interest. To find the best correlation between absorbed bone marrow dose and haematological toxicity it would be valuable to make a multivariate analysis, including all factors known to influence the response. The function of the kidneys as well as the absorbed dose to the kidneys should than be included, as an inferior renal function correlates both to higher renal absorbed doses and haematological toxicity.

To acquire a full understanding of what decides the normal tissue response for the individual patient in ^{177}Lu-DOTATATE treatment, and make the best decision for treatment, clinical background data obviously is needed, besides accurate estimates of the absorbed dose to exposed normal organs. To this is added the individual radiosensitivity. The goal is to have methods to early predict both normal tissue response and efficacy, to utilise this treatment for patients that tolerate it and are helped, and to avoid unnecessary exposure for patients more suited for other treatment.

6 CONCLUSIONS

6.1 Pre-clinical study (I)

^{177}Lu-DOTATATE is reabsorbed and retained in the proximal tubules of the kidney cortex. In this study, nude mice injected with ^{177}Lu-DOTATATE responded biochemically and developed selective morphological changes in the proximal tubules in a dose-dependent manner. Corresponding changes for the animals receiving ^{90}Y-DOTATATE were not observed.

6.2 Clinical studies (II, III, IV)

Patients with inferior renal function were exposed to higher mean absorbed renal dose per administered activity and developed higher grade of haematological toxicity during ^{177}Lu-DOTATATE treatment. This indicates that patients with impaired renal function are at risk of greater exposure of the normal tissue. Residence time of ^{177}Lu in the whole-body, and the tumour burden, also affected haematological toxicity.

The image-based method for bone marrow dosimetry developed in paper III, correlated with haematological toxicity. The results encourage further development of the method to increase the accuracy of absorbed dose estimates and the correlation to haematological response.

In paper IV, a modest correlation was observed between absorbed dose to the spleen and developed haematological toxicity. This supports the possibility that the radiation exposure of the spleen is one of the factors that affect haematological response in ^{177}Lu-DOTATATE treatment.

7 FUTURE PERSPECTIVES

Renal dose estimates for patients were based on assumed homogenous absorbed dose distributions. This is however a simplification as we know that the activity is heterogeneously distributed, with the uptake mainly situated in the proximal tubules of the renal cortex. A more detailed calculation of the absorbed dose to the different parts of the kidneys, as done for the mouse kidneys in the pre-clinical study, would be of interest for improved characterisation of the dose distribution and its correlation with toxicity.

As described earlier, α-emitting ^{213}Bi [33] has also shown tumour response in SSTR-based radionuclide therapy, and further development may be expected, to evaluate its efficacy and safety compared to the established β-emitters ^{177}Lu and ^{90}Y. In search of more effective radionuclides for antitumoural treatment, other β-emitters are being investigated. This includes ^{161}Tb that additionally emits conversion and Auger electrons [34]. ^{161}Tb coupled to folate has been compared to ^{177}Lu in pre-clinical therapy studies, showing superior absorbed tumour doses and more efficiently reduced tumour growth [166]. It would therefore be of interest to compare ^{161}Tb-, and ^{177}Lu-coupled somatostatin analogues for treatment of neuroendocrine tumours.

There is a need for more accurate tools to evaluate the response to treatment, according to safety and efficacy. Some patients will tolerate a large amount of treatment, which gives prerequisites for a longstanding remission of the disease, while others should change to other therapies to avoid serious toxicity or inefficient treatment. Ideal would be to have reliable biomarkers for early prediction of tolerability and tumour response.

A potential biomarker of individual radiosensitivity to complement the estimated absorbed bone marrow dose is FMS-related tyrosine kinase 3-ligand (FLT3-L) [167]. This cytokine stimulates haematopoesis and its blood levels may indicate the recovery of the haematopoetic stem cells after radiation. An improved correlation between bone marrow dose and haematological toxicity was observed when an adjustment from the level of plasma FLT3-L was made in ^{131}I-based radioimmunotherapy [167]. This would be of interest to explore during ^{177}Lu-DOTATATE.

To obtain an individual normal tissue response estimate, a model that includes the factors affecting bone marrow response; renal function, blood counts, renal, bone marrow and spleen dose, tumour burden and bone metastases, would be valuable to develop. To this, biomarkers of normal

tissue response could be added. FLT3-L is one, but the individual radiosensitivity may also be evaluated from weekly blood sampling of Hb, WBC and PLT counts. In Figure 13, the variations in PLT counts during ^{177}Lu-DOTATATE treatment is shown. The shape of the curve illustrates the individual response to treatment and its recovery, and a description of this curve could serve as a tool to make early predictions on bone marrow tolerance. To reveal the individual response pattern and model the response, more frequent sampling is needed to capture the nadir value and the shape of the curve. The ongoing prospective study on ^{177}Lu-DOTATATE (ILUMINET, EudraCT 2011-000240-16) includes blood sampling every week, which gives prerequisites for this modelling.

This thesis is focused on normal tissue response. Future plans also include tumour response evaluations. Traditional imaging for assessment of changes in tumour size is already complemented with functional imaging for tumour response evaluation in general. For NETs, somatostatin analogue-based ^{68}Ga PET/CT is evolving, and early changes in uptake during treatment may have the ability to predict survival. This was reported both after ^{177}Lu-DOTATATE [168] and after hepatic ^{90}Y-microsphere treatment [169]. If response can be evaluated early, patients can be directed to other treatment without unnecessary exposure. It would be of value to include somatostatin analogue-based ^{68}Ga PET/CT for further evaluation of its predictive potential in a future study. This could be complemented with a suitable biomarker for early response prediction, for example the analysis of changes in disease specific gene transcript levels in blood [114].

ACKNOWLEDGEMENTS

This work was supported by grants from the Swedish National Cancer Society, the Swedish Radiation Safety Authority and the Jubilee Clinic Cancer Research Foundation.

First of all, I want to thank my supervisor Peter Bernhardt. You have been such an inspiration from the first day, being a great scientist, coach and friend. You have shown the joy of research in a wide perspective, and I hope that we will continue to work together for a long time.

I would also like to thank my three co-supervisors; Ragnar Hultborn, Per Karlsson and Bo Wängberg, for engagement and valuable input. Gertrud Berg introduced me to radionuclide therapy. I am very greatful for this, and for all your knowledge and encouragement. Thank you co-authors Johan Mölne and Mark Konijnenberg, for important contribution to this work, and for always being enthusiastic. Thank you all members of the PhONSA research group. It is great fun and true inspiration to work with you; Jakob Lagerlöf, Jonas Högberg, Tobias Magnander, Rebecca Hermann, Emma Wikberg and the newest members Linn Hagmarker and Jens Hemmingsson, who made the last six months such a joy.

The isotope-team; Karin, Sara and Amanda, you are extraordinary nurses and always supportive; and my colleagues Helen, Andreas, Fredrik and Ulf, thank you for good teamwork. Kajsa Holgersson; I am thankful for our collaboration, you are such an excellent working partner and a good friend. Thank you MFT; Kirsten, Alexa, Lena, Petra, Ylva, Johanna and Jakobina, and the whole team at the Department of Nuclear Medicine, for all support.

I am also grateful to all friends and colleagues att the Jubilee Clinic, for all warmth, support and all good laughs, that make it a workplace I want to be in. Hedda, I am very happy for having you as my roommate and friend, you are always there for me. And thank you Jan, head of team 4, for being a constant inspiration as a skilled clinical researcher, for believing in me, and for never saying no.

Last but most important, thank you to my family; Anders, Sofia, Julia and Sara. You make my life spin.

REFERENCES

1. Tischler AS. The dispersed neuroendocrine cells: the structure, function, regulation and effects of xenobiotics on this system. Toxicol Pathol. 1989;17:307-16.
2. Oberg K, Knigge U, Kwekkeboom D, Perren A. Neuroendocrine gastro-entero-pancreatic tumors: ESMO Clinical Practice Guidelines for diagnosis, treatment and follow-up. Ann Oncol. 2012;23 Suppl 7:vii124-30.
3. Oberg K, Hellman P, Ferolla P, Papotti M. Neuroendocrine bronchial and thymic tumors: ESMO Clinical Practice Guidelines for diagnosis, treatment and follow-up. Ann Oncol. 2012;23 Suppl 7:vii120-3.
4. Yao JC, Hassan M, Phan A, Dagohoy C, Leary C, Mares JE, et al. One hundred years after "carcinoid": epidemiology of and prognostic factors for neuroendocrine tumors in 35,825 cases in the United States. J Clin Oncol. 2008;26:3063-72.
5. Hallet J, Law CH, Cukier M, Saskin R, Liu N, Singh S. Exploring the rising incidence of neuroendocrine tumors: a population-based analysis of epidemiology, metastatic presentation, and outcomes. Cancer. 2015;121:589-97.
6. Ito T, Igarashi H, Nakamura K, Sasano H, Okusaka T, Takano K, et al. Epidemiological trends of pancreatic and gastrointestinal neuroendocrine tumors in Japan: a nationwide survey analysis. J Gastroenterol. 2015;50:58-64.
7. Lepage C, Bouvier AM, Faivre J. Endocrine tumours: epidemiology of malignant digestive neuroendocrine tumours. Eur J Endocrinol. 2013;168:R77-83.
8. Bosman FT, Organization WH, Cancer IAfRo. WHO classification of tumours of the digestive system. 2010.
9. Tang LH, Gonen M, Hedvat C, Modlin IM, Klimstra DS. Objective quantification of the Ki67 proliferative index in neuroendocrine tumors of the gastroenteropancreatic system: a comparison of digital image analysis with manual methods. Am J Surg Pathol. 2012;36:1761-70.
10. Klimstra DS, Modlin IR, Coppola D, Lloyd RV, Suster S. The pathologic classification of neuroendocrine tumors: a review of nomenclature, grading, and staging systems. Pancreas. 2010;39:707-12.
11. de Baere T, Deschamps F, Tselikas L, Ducreux M, Planchard D, Pearson E, et al. GEP-NETS update: Interventional radiology: role in the treatment of liver metastases from GEP-NETs. Eur J Endocrinol. 2015;172:R151-66.

12. Dilz LM, Denecke T, Steffen IG, Prasad V, von Weikersthal LF, Pape UF, et al. Streptozocin/5-fluorouracil chemotherapy is associated with durable response in patients with advanced pancreatic neuroendocrine tumours. Eur J Cancer. 2015;51:1253-62.
13. Yao JC, Shah MH, Ito T, Bohas CL, Wolin EM, Van Cutsem E, et al. Everolimus for advanced pancreatic neuroendocrine tumors. N Engl J Med. 2011;364:514-23.
14. Raymond E, Dahan L, Raoul JL, Bang YJ, Borbath I, Lombard-Bohas C, et al. Sunitinib malate for the treatment of pancreatic neuroendocrine tumors. N Engl J Med. 2011;364:501-13.
15. Gorden P, Comi RJ, Maton PN, Go VL. NIH conference. Somatostatin and somatostatin analogue (SMS 201-995) in treatment of hormone-secreting tumors of the pituitary and gastrointestinal tract and non-neoplastic diseases of the gut. Ann Intern Med. 1989;110:35-50.
16. Rinke A, Muller HH, Schade-Brittinger C, Klose KJ, Barth P, Wied M, et al. Placebo-controlled, double-blind, prospective, randomized study on the effect of octreotide LAR in the control of tumor growth in patients with metastatic neuroendocrine midgut tumors: a report from the PROMID Study Group. J Clin Oncol. 2009;27:4656-63.
17. Caplin ME, Pavel M, Cwikla JB, Phan AT, Raderer M, Sedlackova E, et al. Lanreotide in metastatic enteropancreatic neuroendocrine tumors. N Engl J Med. 2014;371:224-33.
18. Krenning EP, Kwekkeboom DJ, Bakker WH, Breeman WA, Kooij PP, Oei HY, et al. Somatostatin receptor scintigraphy with [111In-DTPA-D-Phe1]- and [123I-Tyr3]-octreotide: the Rotterdam experience with more than 1000 patients. Eur J Nucl Med. 1993;20:716-31.
19. Hoyer D, Lubbert H, Bruns C. Molecular pharmacology of somatostatin receptors. Naunyn Schmiedebergs Arch Pharmacol. 1994;350:441-53.
20. Reubi JC, Waser B. Concomitant expression of several peptide receptors in neuroendocrine tumours: molecular basis for in vivo multireceptor tumour targeting. Eur J Nucl Med Mol Imaging. 2003;30:781-93.
21. Reubi JC, Hacki WH, Lamberts SW. Hormone-producing gastrointestinal tumors contain a high density of somatostatin receptors. J Clin Endocrinol Metab. 1987;65:1127-34. doi:10.1210/jcem-65-6-1127.
22. Krenning EP, Bakker WH, Breeman WA, Koper JW, Kooij PP, Ausema L, et al. Localisation of endocrine-related tumours with radioiodinated analogue of somatostatin. Lancet. 1989;1:242-4.
23. Lamberts SW, Chayvialle JA, Krenning EP. The visualization of gastroenteropancreatic endocrine tumors. Metabolism. 1992;41:111-5.

24. Kwekkeboom DJ, Kooij PP, Bakker WH, Macke HR, Krenning EP. Comparison of 111In-DOTA-Tyr3-octreotide and 111In-DTPA-octreotide in the same patients: biodistribution, kinetics, organ and tumor uptake. J Nucl Med. 1999;40:762-7.
25. Krenning EP, Kooij PP, Pauwels S, Breeman WA, Postema PT, De Herder WW, et al. Somatostatin receptor: scintigraphy and radionuclide therapy. Digestion. 1996;57 Suppl 1:57-61.
26. Fjalling M, Andersson P, Forssell-Aronsson E, Gretarsdottir J, Johansson V, Tisell LE, et al. Systemic radionuclide therapy using indium-111-DTPA-D-Phe1-octreotide in midgut carcinoid syndrome. J Nucl Med. 1996;37:1519-21.
27. de Jong M, Breeman WA, Bakker WH, Kooij PP, Bernard BF, Hofland LJ, et al. Comparison of (111)In-labeled somatostatin analogues for tumor scintigraphy and radionuclide therapy. Cancer Res. 1998;58:437-41.
28. Reubi JC, Schar JC, Waser B, Wenger S, Heppeler A, Schmitt JS, et al. Affinity profiles for human somatostatin receptor subtypes SST1-SST5 of somatostatin radiotracers selected for scintigraphic and radiotherapeutic use. Eur J Nucl Med. 2000;27:273-82.
29. Kwekkeboom DJ, Bakker WH, Kooij PP, Konijnenberg MW, Srinivasan A, Erion JL, et al. [177Lu-DOTAOTyr3]octreotate: comparison with [111In-DTPAo]octreotide in patients. Eur J Nucl Med. 2001;28:1319-25.
30. De Jong M, Bernard BF, De Bruin E, Van Gameren A, Bakker WH, Visser TJ, et al. Internalization of radiolabelled [DTPA0]octreotide and [DOTA0,Tyr3]octreotide: peptides for somatostatin receptor-targeted scintigraphy and radionuclide therapy. Nucl Med Commun. 1998;19:283-8.
31. Duncan JR, Stephenson MT, Wu HP, Anderson CJ. Indium-111-diethylenetriaminepentaacetic acid-octreotide is delivered in vivo to pancreatic, tumor cell, renal, and hepatocyte lysosomes. Cancer Res. 1997;57:659-71.
32. Andersson P, Forssell-Aronsson E, Johanson V, Wangberg B, Nilsson O, Fjalling M, et al. Internalization of indium-111 into human neuroendocrine tumor cells after incubation with indium-111-DTPA-D-Phe1-octreotide. J Nucl Med. 1996;37:2002-6.
33. Kratochwil C, Giesel FL, Bruchertseifer F, Mier W, Apostolidis C, Boll R, et al. (2)(1)(3)Bi-DOTATOC receptor-targeted alpha-radionuclide therapy induces remission in neuroendocrine tumours refractory to beta radiation: a first-in-human experience. Eur J Nucl Med Mol Imaging. 2014;41:2106-19.
34. Bernhardt P, Benjegard SA, Kolby L, Johanson V, Nilsson O, Ahlman H, et al. Dosimetric comparison of radionuclides for therapy of somatostatin receptor-expressing tumors. Int J Radiat Oncol Biol Phys. 2001;51:514-24.

35. Buchmann I, Henze M, Engelbrecht S, Eisenhut M, Runz A, Schafer M, et al. Comparison of 68Ga-DOTATOC PET and 111In-DTPAOC (Octreoscan) SPECT in patients with neuroendocrine tumours. Eur J Nucl Med Mol Imaging. 2007;34:1617-26.
36. Van Binnebeek S, Vanbilloen B, Baete K, Terwinghe C, Koole M, Mottaghy FM, et al. Comparison of diagnostic accuracy of In-pentetreotide SPECT and Ga-DOTATOC PET/CT: A lesion-by-lesion analysis in patients with metastatic neuroendocrine tumours. Eur Radiol. 2015.
37. Poeppel TD, Binse I, Petersenn S, Lahner H, Schott M, Antoch G, et al. 68Ga-DOTATOC versus 68Ga-DOTATATE PET/CT in functional imaging of neuroendocrine tumors. J Nucl Med. 2011;52:1864-70.
38. Velikyan I, Sundin A, Sorensen J, Lubberink M, Sandstrom M, Garske-Roman U, et al. Quantitative and qualitative intrapatient comparison of 68Ga-DOTATOC and 68Ga-DOTATATE: net uptake rate for accurate quantification. J Nucl Med. 2014;55:204-10. doi:10.2967/jnumed.113.126177.
39. Yang J, Kan Y, Ge BH, Yuan L, Li C, Zhao W. Diagnostic role of Gallium-68 DOTATOC and Gallium-68 DOTATATE PET in patients with neuroendocrine tumors: a meta-analysis. Acta Radiol. 2014;55:389-98.
40. Wild D, Bomanji JB, Benkert P, Maecke H, Ell PJ, Reubi JC, et al. Comparison of 68Ga-DOTANOC and 68Ga-DOTATATE PET/CT within patients with gastroenteropancreatic neuroendocrine tumors. J Nucl Med. 2013;54:364-72.
41. Kabasakal L, Demirci E, Ocak M, Decristoforo C, Araman A, Ozsoy Y, et al. Comparison of (6)(8)Ga-DOTATATE and (6)(8)Ga-DOTANOC PET/CT imaging in the same patient group with neuroendocrine tumours. Eur J Nucl Med Mol Imaging. 2012;39:1271-7.
42. Kayani I, Conry BG, Groves AM, Win T, Dickson J, Caplin M, et al. A comparison of 68Ga-DOTATATE and 18F-FDG PET/CT in pulmonary neuroendocrine tumors. J Nucl Med. 2009;50:1927-32.
43. Has Simsek D, Kuyumcu S, Turkmen C, Sanli Y, Aykan F, Unal S, et al. Can complementary 68Ga-DOTATATE and 18F-FDG PET/CT establish the missing link between histopathology and therapeutic approach in gastroenteropancreatic neuroendocrine tumors? J Nucl Med. 2014;55:1811-7.
44. Kroiss A, Putzer D, Decristoforo C, Uprimny C, Warwitz B, Nilica B, et al. 68Ga-DOTA-TOC uptake in neuroendocrine tumour and healthy tissue: differentiation of physiological uptake and pathological processes in PET/CT. Eur J Nucl Med Mol Imaging. 2013;40:514-23.

45. Eckerman K, Endo A. ICRP Publication 107. Nuclear decay data for dosimetric calculations. Ann ICRP. 2008;38:7-96.

46. http://physics.nist.gov/cgi-bin/Star/edata.pl. Accessed 15 January 2016.

47. O'Donoghue JA, Bardies M, Wheldon TE. Relationships between tumor size and curability for uniformly targeted therapy with beta-emitting radionuclides. J Nucl Med. 1995;36:1902-9.

48. Breeman WA, De Jong M, Visser TJ, Erion JL, Krenning EP. Optimising conditions for radiolabelling of DOTA-peptides with 90Y, 111In and 177Lu at high specific activities. Eur J Nucl Med Mol Imaging. 2003;30:917-20.

49. Pillai MR, Chakraborty S, Das T, Venkatesh M, Ramamoorthy N. Production logistics of 177Lu for radionuclide therapy. Appl Radiat Isot. 2003;59:109-18.

50. Larsson M, Bernhardt P, Svensson JB, Wangberg B, Ahlman H, Forssell-Aronsson E. Estimation of absorbed dose to the kidneys in patients after treatment with 177Lu-octreotate: comparison between methods based on planar scintigraphy. EJNMMI Res. 2012;2:49.

51. Breeman WA, Chan HS, de Zanger RM, Konijnenberg MK, Blois E. Overview of Development and Formulation of 177Lu-DOTA-TATE for PRRT. Current radiopharmaceuticals. 2016;9:8-18.

52. de Jong M, Breeman WA, Bernard BF, van Gameren A, de Bruin E, Bakker WH, et al. Tumour uptake of the radiolabelled somatostatin analogue [DOTA0, TYR3]octreotide is dependent on the peptide amount. Eur J Nucl Med. 1999;26:693-8.

53. Breeman WA, van der Wansem K, Bernard BF, van Gameren A, Erion JL, Visser TJ, et al. The addition of DTPA to [177Lu-DOTA0,Tyr3]octreotate prior to administration reduces rat skeleton uptake of radioactivity. Eur J Nucl Med Mol Imaging. 2003;30:312-5.

54. Kwekkeboom DJ, de Herder WW, Kam BL, van Eijck CH, van Essen M, Kooij PP, et al. Treatment with the radiolabeled somatostatin analog [177 Lu-DOTA 0,Tyr3]octreotate: toxicity, efficacy, and survival. J Clin Oncol. 2008;26:2124-30.

55. Bodei L, Kidd M, Paganelli G, Grana CM, Drozdov I, Cremonesi M, et al. Long-term tolerability of PRRT in 807 patients with neuroendocrine tumours: the value and limitations of clinical factors. Eur J Nucl Med Mol Imaging. 2015;42:5-19.

56. Sabet A, Ezziddin K, Pape UF, Ahmadzadehfar H, Mayer K, Poppel T, et al. Long-term hematotoxicity after peptide receptor radionuclide therapy with 177Lu-octreotate. J Nucl Med. 2013;54:1857-61.

57. Svensson J, Berg G, Wangberg B, Larsson M, Forssell-Aronsson E, Bernhardt P. Renal function affects absorbed dose to the kidneys and haematological toxicity during (1)(7)(7)Lu-DOTATATE treatment. Eur J Nucl Med Mol Imaging. 2015;42:947-55.
58. Sandstrom M, Garske-Roman U, Granberg D, Johansson S, Widstrom C, Eriksson B, et al. Individualized dosimetry of kidney and bone marrow in patients undergoing 177Lu-DOTA-octreotate treatment. J Nucl Med. 2013;54:33-41.
59. Rolleman EJ, Valkema R, de Jong M, Kooij PP, Krenning EP. Safe and effective inhibition of renal uptake of radiolabelled octreotide by a combination of lysine and arginine. Eur J Nucl Med Mol Imaging. 2003;30:9-15.
60. Kwekkeboom DJ, Teunissen JJ, Bakker WH, Kooij PP, de Herder WW, Feelders RA, et al. Radiolabeled somatostatin analog [177Lu-DOTA0,Tyr3]octreotate in patients with endocrine gastroenteropancreatic tumors. J Clin Oncol. 2005;23:2754-62.
61. Bodei L, Cremonesi M, Grana CM, Fazio N, Iodice S, Baio SM, et al. Peptide receptor radionuclide therapy with (1)(7)(7)Lu-DOTATATE: the IEO phase I-II study. Eur J Nucl Med Mol Imaging. 2011;38:2125-35.
62. Garske U, Sandstrom M, Johansson S, Granberg D, Lundqvist H, Lubberink M, et al. Lessons on Tumour Response: Imaging during Therapy with (177)Lu-DOTA-octreotate. A Case Report on a Patient with a Large Volume of Poorly Differentiated Neuroendocrine Carcinoma. Theranostics. 2012;2:459-71.
63. Sgouros G. Dosimetry of internal emitters. J Nucl Med. 2005;46 Suppl 1:18s-27s.
64. Stabin MG, Tagesson M, Thomas SR, Ljungberg M, Strand SE. Radiation dosimetry in nuclear medicine. Appl Radiat Isot. 1999;50:73-87.
65. Gleisner KS, Brolin G, Sundlov A, Mjekiqi E, Ostlund K, Tennvall J, et al. Long-Term Retention of 177Lu/177mLu-DOTATATE in Patients Investigated by gamma-Spectrometry and gamma-Camera Imaging. J Nucl Med. 2015;56:976-84.
66. Sandstrom M, Garske U, Granberg D, Sundin A, Lundqvist H. Individualized dosimetry in patients undergoing therapy with (177)Lu-DOTA-D-Phe (1)-Tyr (3)-octreotate. Eur J Nucl Med Mol Imaging. 2010;37:212-25.
67. Garkavij M, Nickel M, Sjogreen-Gleisner K, Ljungberg M, Ohlsson T, Wingardh K, et al. 177Lu-[DOTA0,Tyr3] octreotate therapy in patients with disseminated neuroendocrine tumors: Analysis of dosimetry with impact on future therapeutic strategy. Cancer. 2010;116:1084-92.

68. Ilan E, Sandstrom M, Wassberg C, Sundin A, Garske-Roman U, Eriksson B, et al. Dose response of pancreatic neuroendocrine tumors treated with peptide receptor radionuclide therapy using 177Lu-DOTATATE. J Nucl Med. 2015;56:177-82.
69. Forrer F, Krenning EP, Kooij PP, Bernard BF, Konijnenberg M, Bakker WH, et al. Bone marrow dosimetry in peptide receptor radionuclide therapy with [177Lu-DOTA(0),Tyr(3)]octreotate. Eur J Nucl Med Mol Imaging. 2009;36:1138-46.
70. Hindorf C, Glatting G, Chiesa C, Linden O, Flux G. EANM Dosimetry Committee guidelines for bone marrow and whole-body dosimetry. Eur J Nucl Med Mol Imaging. 2010;37:1238-50.
71. Sgouros G. Bone marrow dosimetry for radioimmunotherapy: theoretical considerations. J Nucl Med. 1993;34:689-94.
72. Behr TM, Behe M, Sgouros G. Correlation of red marrow radiation dosimetry with myelotoxicity: empirical factors influencing the radiation-induced myelotoxicity of radiolabeled antibodies, fragments and peptides in pre-clinical and clinical settings. Cancer Biother Radiopharm. 2002;17:445-64.
73. Basic anatomical and physiological data for use in radiological protection: reference values. A report of age- and gender-related differences in the anatomical and physiological characteristics of reference individuals. ICRP Publication 89. Ann ICRP. 2002;32:5-265.
74. Jackson PA, Beauregard JM, Hofman MS, Kron T, Hogg A, Hicks RJ. An automated voxelized dosimetry tool for radionuclide therapy based on serial quantitative SPECT/CT imaging. Med Phys. 2013;40:112503.
75. Norrgren K, Svegborn SL, Areberg J, Mattsson S. Accuracy of the quantification of organ activity from planar gamma camera images. Cancer Biother Radiopharm. 2003;18:125-31.
76. Magnander T, Svensson J, Båth M, Gjertsson P, Bernhardt P. Improved planar kidney activity concentration estimate by the posterior-view method in 177Lu-DOTATATE treatments. Radiation Protection Dosimetry. 2016. DOI 10.1093/rpd/ncw046.
77. Pereira JM, Stabin MG, Lima FR, Guimaraes MI, Forrester JW. Image quantification for radiation dose calculations--limitations and uncertainties. Health Phys. 2010;99:688-701.
78. Ritt P, Vija H, Hornegger J, Kuwert T. Absolute quantification in SPECT. Eur J Nucl Med Mol Imaging. 2011;38 Suppl 1:S69-77.
79. Sanders JC, Kuwert T, Hornegger J, Ritt P. Quantitative SPECT/CT Imaging of (177)Lu with In Vivo Validation in Patients Undergoing Peptide Receptor Radionuclide Therapy. Mol Imaging Biol. 2015;17:585-93.
80. Ljungberg M, Celler A, Konijnenberg MW, Eckerman KF, Dewaraja YK, Sjogreen-Gleisner K. MIRD Pamphlet No. 26: Joint

EANM/MIRD Guidelines for Quantitative 177Lu SPECT Applied for Dosimetry of Radiopharmaceutical Therapy. J Nucl Med. 2016;57:151-62.
81. Cremonesi M, Ferrari M, Di Dia A, Botta F, De Cicco C, Bodei L, et al. Recent issues on dosimetry and radiobiology for peptide receptor radionuclide therapy. Q J Nucl Med Mol Imaging. 2011;55:155-67.
82. Helisch A, Forster GJ, Reber H, Buchholz HG, Arnold R, Goke B, et al. Pre-therapeutic dosimetry and biodistribution of 86Y-DOTA-Phe1-Tyr3-octreotide versus 111In-pentetreotide in patients with advanced neuroendocrine tumours. Eur J Nucl Med Mol Imaging. 2004;31:1386-92.
83. Hindorf C, Chittenden S, Causer L, Lewington VJ, Macke HR, Flux GD. Dosimetry for (90)Y-DOTATOC therapies in patients with neuroendocrine tumors. Cancer Biother Radiopharm. 2007;22:130-5.
84. Pauwels S, Barone R, Walrand S, Borson-Chazot F, Valkema R, Kvols LK, et al. Practical dosimetry of peptide receptor radionuclide therapy with (90)Y-labeled somatostatin analogs. J Nucl Med. 2005;46 Suppl 1:92s-8s.
85. Barone R, Borson-Chazot F, Valkema R, Walrand S, Chauvin F, Gogou L, et al. Patient-specific dosimetry in predicting renal toxicity with (90)Y-DOTATOC: relevance of kidney volume and dose rate in finding a dose-effect relationship. J Nucl Med. 2005;46 Suppl 1:99s-106s.
86. Wang L, Tang K, Zhang Q, Li H, Wen Z, Zhang H, et al. Somatostatin receptor-based molecular imaging and therapy for neuroendocrine tumors. Biomed Res Int. 2013;2013:102819.
87. Ezziddin S, Khalaf F, Vanezi M, Haslerud T, Mayer K, Al Zreiqat A, et al. Outcome of peptide receptor radionuclide therapy with 177Lu-octreotate in advanced grade 1/2 pancreatic neuroendocrine tumours. Eur J Nucl Med Mol Imaging. 2014;41:925-33.
88. Teunissen JJ, Kwekkeboom DJ, Krenning EP. Quality of life in patients with gastroenteropancreatic tumors treated with [177Lu-DOTA0,Tyr3]octreotate. J Clin Oncol. 2004;22:2724-9.
89. Vinjamuri S, Gilbert TM, Banks M, McKane G, Maltby P, Poston G, et al. Peptide receptor radionuclide therapy with (90)Y-DOTATATE/(90)Y-DOTATOC in patients with progressive metastatic neuroendocrine tumours: assessment of response, survival and toxicity. Br J Cancer. 2013;108:1440-8.
90. Cwikla JB, Sankowski A, Seklecka N, Buscombe JR, Nasierowska-Guttmejer A, Jeziorski KG, et al. Efficacy of radionuclide treatment DOTATATE Y-90 in patients with progressive metastatic gastroenteropancreatic neuroendocrine carcinomas (GEP-NETs): a phase II study. Ann Oncol. 2010;21:787-94.
91. Kunikowska J, Krolicki L, Hubalewska-Dydejczyk A, Mikolajczak R, Sowa-Staszczak A, Pawlak D. Clinical results of radionuclide

therapy of neuroendocrine tumours with 90Y-DOTATATE and tandem 90Y/177Lu-DOTATATE: which is a better therapy option? Eur J Nucl Med Mol Imaging. 2011;38:1788-97.
92. Reubi JC, Waser B, Horisberger U, Krenning E, Lamberts SW, Gebbers JO, et al. In vitro autoradiographic and in vivo scintigraphic localization of somatostatin receptors in human lymphatic tissue. Blood. 1993;82:2143-51.
93. de Jong M, Barone R, Krenning E, Bernard B, Melis M, Visser T, et al. Megalin is essential for renal proximal tubule reabsorption of (111)In-DTPA-octreotide. J Nucl Med. 2005;46:1696-700.
94. Melis M, Krenning EP, Bernard BF, Barone R, Visser TJ, de Jong M. Localisation and mechanism of renal retention of radiolabelled somatostatin analogues. Eur J Nucl Med Mol Imaging. 2005;32:1136-43.
95. De Jong M, Valkema R, Van Gameren A, Van Boven H, Bex A, Van De Weyer EP, et al. Inhomogeneous localization of radioactivity in the human kidney after injection of [(111)In-DTPA]octreotide. J Nucl Med. 2004;45:1168-71.
96. Bhandari S, Watson N, Long E, Sharpe S, Zhong W, Xu SZ, et al. Expression of somatostatin and somatostatin receptor subtypes 1-5 in human normal and diseased kidney. J Histochem Cytochem. 2008;56:733-43.
97. Unger N, Ueberberg B, Schulz S, Saeger W, Mann K, Petersenn S. Differential expression of somatostatin receptor subtype 1-5 proteins in numerous human normal tissues. Exp Clin Endocrinol Diabetes. 2012;120:482-9.
98. Emami B, Lyman J, Brown A, Coia L, Goitein M, Munzenrider JE, et al. Tolerance of normal tissue to therapeutic irradiation. Int J Radiat Oncol Biol Phys. 1991;21:109-22.
99. Fowler JF. Review: total doses in fractionated radiotherapy--implications of new radiobiological data. Int J Radiat Biol Relat Stud Phys Chem Med. 1984;46:103-20.
100. Dale R. Use of the linear-quadratic radiobiological model for quantifying kidney response in targeted radiotherapy. Cancer Biother Radiopharm. 2004;19:363-70.
101. Valkema R, Pauwels SA, Kvols LK, Kwekkeboom DJ, Jamar F, de Jong M, et al. Long-term follow-up of renal function after peptide receptor radiation therapy with (90)Y-DOTA(0),Tyr(3)-octreotide and (177)Lu-DOTA(0), Tyr(3)-octreotate. J Nucl Med. 2005;46 Suppl 1:83S-91S.
102. Bodei L, Cremonesi M, Ferrari M, Pacifici M, Grana CM, Bartolomei M, et al. Long-term evaluation of renal toxicity after peptide receptor radionuclide therapy with 90Y-DOTATOC and 177Lu-DOTATATE: the role of associated risk factors. Eur J Nucl Med Mol Imaging. 2008;35:1847-56.

103. Sabet A, Ezziddin K, Pape UF, Reichman K, Haslerud T, Ahmadzadehfar H, et al. Accurate assessment of long-term nephrotoxicity after peptide receptor radionuclide therapy with (177)Lu-octreotate. Eur J Nucl Med Mol Imaging. 2014;41:505-10.
104. Imhof A, Brunner P, Marincek N, Briel M, Schindler C, Rasch H, et al. Response, survival, and long-term toxicity after therapy with the radiolabeled somatostatin analogue [90Y-DOTA]-TOC in metastasized neuroendocrine cancers. J Clin Oncol. 2011;29:2416-23.
105. Nonstochastic effects of ionizing radiation. Ann ICRP. 1984;14:1-33.
106. Benua RS, Cicale NR, Sonenberg M, Rawson RW. The relation of radioiodine dosimetry to results and complications in the treatment of metastatic thyroid cancer. Am J Roentgenol Radium Ther Nucl Med. 1962;87:171-82.
107. Lassmann M, Hanscheid H, Chiesa C, Hindorf C, Flux G, Luster M. EANM Dosimetry Committee series on standard operational procedures for pre-therapeutic dosimetry I: blood and bone marrow dosimetry in differentiated thyroid cancer therapy. Eur J Nucl Med Mol Imaging. 2008;35:1405-12.
108. Bergsma H, Konijnenberg MW, Kam BL, Teunissen JJ, Kooij PP, de Herder WW, et al. Subacute haematotoxicity after PRRT with (177)Lu-DOTA-octreotate: prognostic factors, incidence and course. Eur J Nucl Med Mol Imaging. 2016;43:453-63.
109. Eberlein U, Nowak C, Bluemel C, Buck AK, Werner RA, Scherthan H, et al. DNA damage in blood lymphocytes in patients after (177)Lu peptide receptor radionuclide therapy. Eur J Nucl Med Mol Imaging. 2015;42:1739-49.
110. Denoyer D, Lobachevsky P, Jackson P, Thompson M, Martin OA, Hicks RJ. Analysis of 177Lu-DOTA-octreotate therapy-induced DNA damage in peripheral blood lymphocytes of patients with neuroendocrine tumors. J Nucl Med. 2015;56:505-11.
111. Willers H, Gheorghiu L, Liu Q, Efstathiou JA, Wirth LJ, Krause M, et al. DNA Damage Response Assessments in Human Tumor Samples Provide Functional Biomarkers of Radiosensitivity. Semin Radiat Oncol. 2015;25:237-50.
112. Leatherbarrow EL, Harper JV, Cucinotta FA, O'Neill P. Induction and quantification of gamma-H2AX foci following low and high LET-irradiation. Int J Radiat Biol. 2006;82:111-8.
113. Modlin IM, Frilling A, Salem RR, Alaimo D, Drymousis P, Wasan HS, et al. Blood measurement of neuroendocrine gene transcripts defines the effectiveness of operative resection and ablation strategies. Surgery. 2016;159:336-47.
114. Bodei L, Kidd M, Modlin IM, Severi S, Drozdov I, Nicolini S, et al. Measurement of circulating transcripts and gene cluster analysis predicts and defines therapeutic efficacy of peptide receptor

radionuclide therapy (PRRT) in neuroendocrine tumors. Eur J Nucl Med Mol Imaging. 2015.
115. Cwikla JB, Bodei L, Kolasinska-Cwikla A, Sankowski A, Modlin IM, Kidd M. Circulating Transcript Analysis (NETest) in GEP-NETs Treated With Somatostatin Analogs Defines Therapy. J Clin Endocrinol Metab. 2015;100:E1437-45.
116. Bernhardt P, Oddstig J, Kolby L, Nilsson O, Ahlman H, Forssell-Aronsson E. Effects of treatment with (177)Lu-DOTA-Tyr(3)-octreotate on uptake of subsequent injection in carcinoid-bearing nude mice. Cancer Biother Radiopharm. 2007;22:644-53.
117. Melis M, Forrer F, Capello A, Bijster M, Bernard BF, Reubi JC, et al. Up-regulation of somatostatin receptor density on rat CA20948 tumors escaped from low dose [177Lu-DOTA0,Tyr3]octreotate therapy. Q J Nucl Med Mol Imaging. 2007;51:324-33.
118. Oddstig J, Bernhardt P, Nilsson O, Ahlman H, Forssell-Aronsson E. Radiation-induced up-regulation of somatostatin receptor expression in small cell lung cancer in vitro. Nucl Med Biol. 2006;33:841-6.
119. Dalm SU, Nonnekens J, Doeswijk GN, de Blois E, van Gent DC, Konijnenberg MW, et al. Comparison of the Therapeutic Response to Treatment with a 177Lu-Labeled Somatostatin Receptor Agonist and Antagonist in Preclinical Models. J Nucl Med. 2016;57:260-5.
120. Wild D, Fani M, Fischer R, Del Pozzo L, Kaul F, Krebs S, et al. Comparison of somatostatin receptor agonist and antagonist for peptide receptor radionuclide therapy: a pilot study. J Nucl Med. 2014;55:1248-52. doi:10.2967/jnumed.114.138834.
121. Vegt E, de Jong M, Wetzels JF, Masereeuw R, Melis M, Oyen WJ, et al. Renal toxicity of radiolabeled peptides and antibody fragments: mechanisms, impact on radionuclide therapy, and strategies for prevention. J Nucl Med. 2010;51:1049-58.
122. Vegt E, Wetzels JF, Russel FG, Masereeuw R, Boerman OC, van Eerd JE, et al. Renal uptake of radiolabeled octreotide in human subjects is efficiently inhibited by succinylated gelatin. J Nucl Med. 2006;47:432-6.
123. Gotthardt M, van Eerd-Vismale J, Oyen WJ, de Jong M, Zhang H, Rolleman E, et al. Indication for different mechanisms of kidney uptake of radiolabeled peptides. J Nucl Med. 2007;48:596-601.
124. Olsson MG, Nilsson EJ, Rutardottir S, Paczesny J, Pallon J, Akerstrom B. Bystander cell death and stress response is inhibited by the radical scavenger alpha(1)-microglobulin in irradiated cell cultures. Radiat Res. 2010;174:590-600.
125. Ahlstedt J, Tran TA, Strand F, Holmqvist B, Strand SE, Gram M, et al. Biodistribution and pharmacokinetics of recombinant alpha1-microglobulin and its potential use in radioprotection of kidneys. Am J Nucl Med Mol Imaging. 2015;5:333-47.

126. Sabet A, Nagarajah J, Dogan AS, Biersack HJ, Sabet A, Guhlke S, et al. Does PRRT with standard activities of 177Lu-octreotate really achieve relevant somatostatin receptor saturation in target tumor lesions?: insights from intra-therapeutic receptor imaging in patients with metastatic gastroenteropancreatic neuroendocrine tumors. EJNMMI Res. 2013;3:82.
127. Velikyan I, Sundin A, Eriksson B, Lundqvist H, Sorensen J, Bergstrom M, et al. In vivo binding of [68Ga]-DOTATOC to somatostatin receptors in neuroendocrine tumours--impact of peptide mass. Nucl Med Biol. 2010;37:265-75.
128. Pool SE, Krenning EP, Koning GA, van Eijck CH, Teunissen JJ, Kam B, et al. Preclinical and clinical studies of peptide receptor radionuclide therapy. Semin Nucl Med. 2010;40:209-18.
129. Christ E, Wild D, Forrer F, Brandle M, Sahli R, Clerici T, et al. Glucagon-like peptide-1 receptor imaging for localization of insulinomas. J Clin Endocrinol Metab. 2009;94:4398-405.
130. Velikyan I, Bulenga TN, Selvaraju R, Lubberink M, Espes D, Rosenstrom U, et al. Dosimetry of [(177)Lu]-DO3A-VS-Cys(40)-Exendin-4 - impact on the feasibility of insulinoma internal radiotherapy. Am J Nucl Med Mol Imaging. 2015;5:109-26.
131. Weibel E. Stereological Methods. Academic Press, London. 1979.
132. ICRU Report 46. Photon, Electron, Proton and Neutron Interaction Data for Body Tissues. 1992.
133. Eckerman Keith F EA. MIRD: Radionuclide Data and Decay Schemes. SNM Publication. 2008.
134. Kolby L, Bernhardt P, Johanson V, Schmitt A, Ahlman H, Forssell-Aronsson E, et al. Successful receptor-mediated radiation therapy of xenografted human midgut carcinoid tumour. Br J Cancer. 2005;93:1144-51.
135. Magnander T, Wikberg E, Svensson J, Gjertsson P, Wangberg B, Bath M, et al. A novel statistical analysis method to improve the detection of hepatic foci of (111)In-octreotide in SPECT/CT imaging. EJNMMI physics. 2016;3:1.
136. http://doseinfo-radar.com/. Accessed December 7 2015.
137. Melis M, Krenning EP, Bernard BF, de Visser M, Rolleman E, de Jong M. Renal uptake and retention of radiolabeled somatostatin, bombesin, neurotensin, minigastrin and CCK analogues: species and gender differences. Nucl Med Biol. 2007;34:633-41.
138. Levey AS, Coresh J. Chronic kidney disease. Lancet. 2012;379:165-80.
139. Delanaye P, Schaeffner E, Ebert N, Cavalier E, Mariat C, Krzesinski JM, et al. Normal reference values for glomerular filtration rate: what do we really know? Nephrol Dial Transplant. 2012;27:2664-72.

140. Weinstein JR, Anderson S. The aging kidney: physiological changes. Adv Chronic Kidney Dis. 2010;17:302-7.
141. Herget-Rosenthal S, Bokenkamp A, Hofmann W. How to estimate GFR-serum creatinine, serum cystatin C or equations? Clin Biochem. 2007;40:153-61.
142. Hobbs RF, Song H, Huso DL, Sundel MH, Sgouros G. A nephron-based model of the kidneys for macro-to-micro alpha-particle dosimetry. Phys Med Biol. 2012;57:4403-24.
143. Rolleman EJ, Krenning EP, Bernard BF, de Visser M, Bijster M, Visser TJ, et al. Long-term toxicity of [(177)Lu-DOTA (0),Tyr (3)]octreotate in rats. Eur J Nucl Med Mol Imaging. 2007;34:219-27.
144. Christensen EI, Gburek J. Protein reabsorption in renal proximal tubule-function and dysfunction in kidney pathophysiology. Pediatr Nephrol. 2004;19:714-21.
145. He B, Du Y, Segars WP, Wahl RL, Sgouros G, Jacene H, et al. Evaluation of quantitative imaging methods for organ activity and residence time estimation using a population of phantoms having realistic variations in anatomy and uptake. Med Phys. 2009;36:612-9.
146. Dewaraja YK, Frey EC, Sgouros G, Brill AB, Roberson P, Zanzonico PB, et al. MIRD pamphlet No. 23: quantitative SPECT for patient-specific 3-dimensional dosimetry in internal radionuclide therapy. J Nucl Med. 2012;53:1310-25.
147. Durand E, Prigent A. The basics of renal imaging and function studies. Q J Nucl Med. 2002;46:249-67.
148. Weyer K, Nielsen R, Petersen SV, Christensen EI, Rehling M, Birn H. Renal uptake of 99mTc-dimercaptosuccinic acid is dependent on normal proximal tubule receptor-mediated endocytosis. J Nucl Med. 2013;54:159-65.
149. Durand E, Chaumet-Riffaud P, Grenier N. Functional renal imaging: new trends in radiology and nuclear medicine. Semin Nucl Med. 2011;41:61-72.
150. Forrer F, Rolleman E, Bijster M, Melis M, Bernard B, Krenning EP, et al. From outside to inside? Dose-dependent renal tubular damage after high-dose peptide receptor radionuclide therapy in rats measured with in vivo (99m)Tc-DMSA-SPECT and molecular imaging. Cancer Biother Radiopharm. 2007;22:40-9.
151. Grubb A, Christensson A. [Time for new measurements in kidney disease diagnosis and follow-up]. Lakartidningen. 2013;110:1021-4.
152. Guerriero F, Ferrari ME, Botta F, Fioroni F, Grassi E, Versari A, et al. Kidney dosimetry in (1)(7)(7)Lu and (9)(0)Y peptide receptor radionuclide therapy: influence of image timing, time-activity integration method, and risk factors. Biomed Res Int. 2013;2013:935351.

153. Panjeta M, Tahirovic I, Karamehic J, Sofic E, Ridic O, Coric J. The Relation of Erythropoietin Towards Hemoglobin and Hematocrit in Varying Degrees of Renal Insufficiency. Materia socio-medica. 2015;27:144-8.
154. Kam BL, Teunissen JJ, Krenning EP, de Herder WW, Khan S, van Vliet EI, et al. Lutetium-labelled peptides for therapy of neuroendocrine tumours. Eur J Nucl Med Mol Imaging. 2012;39 Suppl 1:S103-12.
155. Garske U, Sandstrom M, Johansson S, Sundin A, Granberg D, Eriksson B, et al. Minor changes in effective half-life during fractionated 177Lu-octreotate therapy. Acta Oncol. 2012;51:86-96.
156. Wehrmann C, Senftleben S, Zachert C, Muller D, Baum RP. Results of individual patient dosimetry in peptide receptor radionuclide therapy with 177Lu DOTA-TATE and 177Lu DOTA-NOC. Cancer Biother Radiopharm. 2007;22:406-16.
157. Hindorf C, Linden O, Tennvall J, Wingardh K, Strand SE. Time dependence of the activity concentration ratio of red marrow to blood and implications for red marrow dosimetry. Cancer. 2002;94:1235-9.
158. Siegel JA, Lee RE, Pawlyk DA, Horowitz JA, Sharkey RM, Goldenberg DM. Sacral scintigraphy for bone marrow dosimetry in radioimmunotherapy. Int J Rad Appl Instrum B. 1989;16:553-9.
159. Justesen J, Stenderup K, Ebbesen EN, Mosekilde L, Steiniche T, Kassem M. Adipocyte tissue volume in bone marrow is increased with aging and in patients with osteoporosis. Biogerontology. 2001;2:165-71.
160. Kulkarni HR, Prasad V, Schuchardt C, Baum RP. Is there a correlation between peptide receptor radionuclide therapy-associated hematological toxicity and spleen dose? Recent Results Cancer Res. 2013;194:561-6.
161. Shrimali RK, Correa PD, O'Rourke N. Low-dose palliative splenic irradiation in haematolymphoid malignancy. J Med Imaging Radiat Oncol. 2008;52:297-302.
162. Kriz J, Micke O, Bruns F, Haverkamp U, Mucke R, Schafer U, et al. Radiotherapy of splenomegaly : a palliative treatment option for a benign phenomenon in malignant diseases. Strahlenther Onkol. 2011;187:221-4.
163. Pistevou-Gombaki K, Zygogianni A, Kantzou I, Kyrgias G, Mystakidou K, Kouvaris J, et al. Splenic irradiation as palliative treatment for symptomatic splenomegaly due to secondary myelofibrosis: a multi-institutional experience. J BUON. 2015;20:1132-6.
164. Betty C. Hematology in practice. 2 ed: F.A. Davis Company, Philadelphia, PA 19103; 2012.

165. Lavrenkov K, Krepel-Volsky S, Levi I, Ariad S. Low dose palliative radiotherapy for splenomegaly in hematologic disorders. Leuk Lymphoma. 2012;53:430-4.
166. Muller C, Reber J, Haller S, Dorrer H, Bernhardt P, Zhernosekov K, et al. Direct in vitro and in vivo comparison of (161)Tb and (177)Lu using a tumour-targeting folate conjugate. Eur J Nucl Med Mol Imaging. 2014;41:476-85.
167. Siegel JA, Yeldell D, Goldenberg DM, Stabin MG, Sparks RB, Sharkey RM, et al. Red marrow radiation dose adjustment using plasma FLT3-L cytokine levels: improved correlations between hematologic toxicity and bone marrow dose for radioimmunotherapy patients. J Nucl Med. 2003;44:67-76.
168. Haug AR, Auernhammer CJ, Wangler B, Schmidt GP, Uebleis C, Goke B, et al. 68Ga-DOTATATE PET/CT for the early prediction of response to somatostatin receptor-mediated radionuclide therapy in patients with well-differentiated neuroendocrine tumors. J Nucl Med. 2010;51:1349-56.
169. Filippi L, Scopinaro F, Pelle G, Cianni R, Salvatori R, Schillaci O, et al. Molecular response assessed by (68)Ga-DOTANOC and survival after (90)Y microsphere therapy in patients with liver metastases from neuroendocrine tumours. Eur J Nucl Med Mol Imaging. 2016;43:432-40.